


Yi-Qi-Xuan-Fei Formula ameliorate chronic obstructive pulmonary disease by remodeling lung and intestinal florase in rat models

Follow this and additional works at: <https://www.jfda-online.com/journal>

 Part of the [Food Science Commons](#), [Medicinal Chemistry and Pharmaceutics Commons](#), [Pharmacology Commons](#), and the [Toxicology Commons](#)



This work is licensed under a [Creative Commons Attribution-Noncommercial-No Derivative Works 4.0 License](#).

Recommended Citation

Han, Si-Si; Song, Li-Yun; Liang, Peng-Tao; Wang, Yin-Ying; Ying, Yi; Chen, Xiao-Feng; Li, Li; Yuan, Jia-Li; and Yang, Zhong-Shan (2025) "Yi-Qi-Xuan-Fei Formula ameliorate chronic obstructive pulmonary disease by remodeling lung and intestinal florase in rat models," *Journal of Food and Drug Analysis*: Vol. 33 : Iss. 3 , Article 6.
Available at: <https://doi.org/10.38212/2224-6614.3551>

This Original Article is brought to you for free and open access by Journal of Food and Drug Analysis. It has been accepted for inclusion in Journal of Food and Drug Analysis by an authorized editor of Journal of Food and Drug Analysis.

Yi-Qi-Xuan-Fei Formula ameliorate chronic obstructive pulmonary disease by remodeling lung and intestinal flora in rat models

Cover Page Footnote

This work was funded in part by a grant from the National Natural Science Foundation of China (82360017), a grant from Yunnan Provincial Science and Technology Department (202101AZ070001-012, 202201AS070084, 202301AZ070001-004, YNWR- QNBJ-2019-069, 202403AC100007), the central government guides local funds for scientific and technological development (202407AB110020).

Yi-Qi-Xuan-Fei Formula ameliorate chronic obstructive pulmonary disease by remodeling lung and intestinal florase in rat models

Si-Si Han ^{a,b,1}, Li-Yun Song ^{a,1}, Peng-Tao Liang ^{a,1}, Yin-Ying Wang ^a, Yi Ying ^{a,c}, Li Li ^a, Jia-Li Yuan ^{a,**}, Zhong-Shan Yang ^{a,*}

^a Yunnan Key Laboratory of Integrated Traditional Chinese and Western Medicine for Chronic Disease Prevention and Control, Yunnan University of Chinese Medicine, Kunming, 650500, China

^b South China Hospital, Shenzhen University, Shenzhen, 518116, China

^c Department of Pharmacology, School of Basic Medical Sciences, Peking University, Beijing, 100089, China

Abstract

Chronic obstructive pulmonary disease (COPD) is a chronic respiratory disease characterized by various pathological lesions and an imbalance in the microflora. The Yi-Qi-Xuan-Fei Formula (YQXF) is a clinically effective formula with pharmacological potential to delay the progression of COPD. This study aims to explore the relationship between the therapeutic mechanism of YQXF and the microflora in COPD. Our study found that YQXF reduces inflammatory injury and inflammatory cell infiltration in lung tissue, repairs the intestinal mucosal barrier, and enhances immune function. Additionally, YQXF regulates the pulmonary and intestinal flora by increasing the abundance of *Alloprevotella*, *Roseburia*, *Oscillibacter*, and *Lactobacillus*, while reducing the abundance of *Fusobacterium*, *Escherichia/Shigella*, and *Clostridium sensu stricto*. Moreover, YQXF elevates the levels of short-chain fatty acids, which are produced by the intestinal flora. In conclusion, our findings demonstrate that YQXF reduces inflammation levels in lung tissue and repairs the intestinal barrier in COPD rats. Furthermore, the anti-inflammatory and tissue damage prevention effects of YQXF are based on its intervention in the pulmonary and intestinal flora. These findings provide valuable insights into the fundamental mechanism of the herbal formula YQXF and suggest that specifically targeting the intestinal flora could be a potential therapeutic approach for COPD.

Keywords: Chronic obstructive pulmonary disease, Inflammation, Intestinal mucosal barrier, Lung and intestinal flora, Short-chain fatty acids

1. Introduction

Chronic obstructive pulmonary disease (COPD) is a respiratory disease characterized by persistent airflow restriction. The clinical manifestations of this disease include cough, phlegm, chest tightness, shortness of breath, and dyspnea. Additionally, individuals with COPD often experience comorbidities such as cardiovascular disease [1], diabetes [2], osteoporosis [3], and anxiety [4].

Globally, the prevalence of COPD is increasing, presenting considerable threats to public health and imposing significant economic burdens on society. The occurrence, frequency, and fatality rates of COPD vary across countries and regions. Research studies have indicated that the Americas have the highest prevalence of COPD, while Southeast Asia has the lowest. The Mediterranean region has witnessed the fastest growth rate, followed by Africa, whereas Europe has experienced the slowest growth. According to the most recent data

Received 27 October 2024; accepted 3 June 2025.
Available online 18 September 2025

* Corresponding author.

** Corresponding author.

E-mail addresses: Yuanjiali2022521@126.com (J.-L. Yuan), yangzhongshan@ynucm.edu.cn (Z.-S. Yang).

¹ These authors contributed equally to this work.

<https://doi.org/10.38212/2224-6614.3551>

2224-6614/© 2025 Taiwan Food and Drug Administration. This is an open access article under the CC-BY-NC-ND license (<http://creativecommons.org/licenses/by-nc-nd/4.0/>).

published by the World Health Organization (WHO) in 2023, COPD has emerged as the third leading cause of mortality globally. The principal risk factors associated with the development of COPD include smoking and air pollution. The disease exhibits significant heterogeneity in terms of its onset and progression, necessitating tailored clinical regimens. The Global Initiative for COPD recommends the use of glucocorticoids and bronchodilators to reduce inflammation levels and bronchospasm [5]. COPD can be caused by smoking or long-term exposure to harmful substances. However, current treatment methods are associated with common adverse reactions such as increased risk of allergies and disruption of gut microbiota. This has prompted researchers to explore new perspectives and approaches for COPD treatment.

In recent years, numerous studies have confirmed the correlation between abnormal intestinal flora and the occurrence and development of various human diseases, metabolic [6], mental [7], and immune [8] diseases. It has been observed that microorganisms not only exist in the upper respiratory tract but also in the lower respiratory tract, including the lungs. Despite the lack of direct anatomical connection between the lungs and the gut, the composition of the gut microbiota affects the respiratory system through the common mucosal immune system. Similarly, disturbances in the respiratory tract flora can also impact the digestive tract through immune regulation. This interaction is referred to as the “lung-gut axis.” Disruptions in the flora colonized in this axis have been found to influence the occurrence of COPD and other respiratory diseases [9]. Conversely, the administration of probiotics and fecal microbiota transplantation has been shown to modulate the Th1/Th2 and Th17/Treg ratios, consequently attenuating the inflammatory response in murine pulmonary tissue [10]. Therefore, it can be concluded that remodeling the lung and intestinal flora may alleviate COPD.

According to the theory of the “lung-gut axis,” recent Traditional Chinese Medicine (TCM) research has investigated how several classical TCM formulae treat lung diseases. At a systemic pharmacological level, Xuanbai Chengqi decoction has been found to alleviate viral pneumonia caused by different respiratory viruses by inhibiting intestinal immune damage and remodeling intestinal flora [11]. The Qilongtian capsule has been shown to retard the progression of bleomycin-induced pulmonary fibrosis in murine models through the modulation of intestinal microbiota [12]. Additionally, Jianpi Huatan Tongfu granule can alter the

intestinal microflora of patients with acute exacerbation of chronic obstructive pulmonary disease (AECOPD) and reduce pulmonary inflammation [13].

The Yi-Qi-Xuan-Fei Formula (YQXF) is a TCM formula used for the treatment of various respiratory diseases. This formula is an optimized combination based on Yu-Ping-Feng Powder and consists of 11 different medicinal herbs, including *Astragalus*, *Atractylodes macrocephala* Koidz, *Saposhnikovia*, *Fritillaria thunbergii*, *Semen Sinapis*, *Portulaca oleracea*, *Panax notoginseng*, *Curcuma zedoaria* rhizomes, *Rhodiola rosea*, *Draba nemorosa*, and *Folium Alstoniae Scholaris*. These herbs have been proven effective for various lung diseases, including allergic rhinitis [14], chemotherapy-resistant lung cancer [15], bronchial asthma [16], and lung injury [17]. Recent pharmacological research has elucidated the potential of *Astragalus polysaccharides* in mitigating bleomycin-induced pulmonary fibrosis through the modulation of gut microbiota [18]. In addition, *Rhodiola rosea* L. has shown promise in mitigating cigarette smoke and lipopolysaccharide (LPS)-induced COPD in rats through its anti-inflammatory and antioxidant properties [19]. The primary active component, total glycosides of *Rhodiola*, exhibits a protective effect against acute lung injury [20]. Furthermore, Beimu total alkaloids have been found to improve chronic asthma [21] and pulmonary fibrosis [22], while *Sanqi* total saponins have shown a protective effect against pulmonary fibrosis [23] and acute lung injury [24]. Another compound, Baizhu lactone III, not only offers protection against lung injury [25] but also reduces bleomycin-induced pulmonary fibrosis [26] and inflammation levels in asthmatic mice induced by ovalbumin [27]. Curcumin has the potential to enhance inflammatory status and respiratory indicators in individuals diagnosed with severe chronic obstructive pulmonary disease [28].

In our previous study, we found that Yifei Sanjie Formula can alleviate COPD by reshaping the lung microbiota and reducing inflammatory signaling [29]. Furthermore, Yifei Sanjie Formula [30], Curcumin, Curcumol [31], and Astragaloside [32,33] have shown beneficial effects in reducing pulmonary fibrosis by activating autophagy pathways. These data indicate that YQXF has great potential for the treatment of COPD.

The relationship between the lung and gut microbiota and their impact on the development and progression of COPD has been partially confirmed. Our aim is to provide evidence for the therapeutic effects and mechanisms of YQXF in the occurrence and development of COPD. In this study, we used LPS combined with cigarette smoke-

induced COPD rats as a research model and found that YQXF may alleviate pulmonary symptoms in COPD rats by reshaping the gut and respiratory microbiota.

2. Materials and methods

2.1. Extract preparation of YQXF

YQXF is a traditional Chinese herbal formula composed of 11 types of TCM, including *Astragalus*, *Atractylodes macrocephala* Koidz, *Saposhnikovia*, *Fritillaria thunbergii*, *Semen Sinapis*, *Portulaca oleracea*, *Panax notoginseng*, *Curcuma zedoaria* rhizomes, *Rhodiola rosea*, *Draba nemorosa*, and *Folium Alstoniae Scholaris*. The total amount of YQXF is 167 g, and its medicinal ingredients have been identified by Yunnan University of Chinese Medicine. The medicinal herbs undergo a triple boiling process in distilled water, after which the aqueous extract is subjected to filtration and subsequent evaporation under reduced pressure at a temperature of 55 °C. The resulting residue is freeze-dried and stored. The conversion coefficient recommended by the US Food and Drug Administration for rats to humans is 0.018. Based on the equivalent dose of body surface area between humans and rats, the dose for the medium dose group is 15 g/kg/d. In a 1:2:4 ratio, the doses for the low-dose group and the high-dose group are 7.5 g/kg/d and 30 g/kg/d, respectively. The dose concentrations for each group are 1.5 g/mL, 3 g/mL, and 6 g/mL, respectively, when administered by gavage of 1 mL per rat per day. Before gavage, the drug should be adjusted to the corresponding dosing concentration with distilled liquid, and a 0.22 µM filter should be used for backup.

2.2. Animals and treatment

The study was conducted in accordance with the Basic & Clinical Pharmacology & Toxicology policy for experimental studies [34]. Male rats weighing 200 ± 10 g were obtained from Chengdu Dashuo Experimental Animal Co., Ltd. (Experimental Animal Quality Certificate: SCXK (Sichuan) 2020-030). The rats were housed in a temperature-controlled environment (20–24 °C) with a 12-h light/dark cycle and pathogen-free conditions, following the guidelines set by the Commission and the National Institutes of Health, particularly the Guidelines for the Care and Use of Laboratory Animals. The animal experiment was approved by the Animal Experiment Ethics Committee of Yunnan University of Chinese Medicine (Ethics Review Number: R-

06202023, Experimental Animal Use License Number: SYXK (Yunnan) K2017-0005).

In this study, we established a rat model of chronic obstructive pulmonary disease (COPD) by administering lipopolysaccharide (LPS) (Sigma, L2630, USA) and exposing the rats to cigarette smoke. On day 1 and day 14 of the experiment, rats were anesthetized and underwent tracheotomy followed by intratracheal administration of LPS at a dose of 1 g/kg in a volume of 100 µL prepared in normal saline. The control group received the same dose of normal saline. After intratracheal instillation, both the model group and YQXF group were exposed to cigarette smoke (Yunnan Tobacco Company, Kunming, China) twice a day for 30 min each time. In addition, from day 57 to day 84, the YQXF group received daily oral gavage of 1 mL of the drug, while the model group and blank group received an equal volume of normal saline. The rats' body weight and condition were measured and recorded daily, with mortality also being recorded promptly. The rats had free access to food and water.

2.3. Hematoxylin-Eosin (HE) staining

The right upper lobe of the rat lung was surgically removed and fixed in 4% paraformaldehyde for over 24 h. After removing excess fat and connective tissue, the lung tissue was cut into small pieces with a scalpel. Each piece of cut tissue was placed in an embedding frame and labeled with a pencil. The trimmed lung tissue was then immersed in a series of alcohol solutions, starting with 75% alcohol for 4 h, followed by 85% alcohol for 2 h, 90% alcohol for 2 h, 95% alcohol for 1 h, absolute ethanol for 30 min, and finally alcohol benzene for 6 min, and xylene I for 6 min. The tissues were dehydrated with xylene II for 6 min, followed by 65 °C paraffin I for 1 h, 65 °C paraffin II for 1 h, and 65 °C paraffin III for 1 h. Once the paraffin embedding process was completed using an embedding machine, the tissue was cooled on a –20 °C freezer table. After cooling, the tissue was cut into 5 µM sections using a microtome and flattened in warm water at 40 °C using a spreader. The flattened tissues were then placed on slides and baked in an oven at 60 °C. After drying, the sections were washed with xylene (twice for 20 min each), absolute ethanol (twice for 5 min each), 75% alcohol (once for a total of 5 min), and finally with tap water. The sections were stained with hematoxylin staining solution for 5 min, followed by dehydration, differentiation, back blue, and eosin staining solution for an additional 5 min. The stained tissue sections were then dehydrated,

transparent, sealed with neutral gum, and examined under a microscope.

2.4. Immunohistochemistry (IHC)

Tissue sections were dewaxed using xylene and gradient ethanol. They were then placed in citrate antigen repair buffer (pH = 6.0) for antigen repair. The slices were treated with 3% hydrogen peroxide solution to quench endogenous peroxidase and incubated at room temperature in the dark for 25 min. To ensure even coverage, the tissues were incubated with a 3% bovine serum albumin solution (Servicebio, G5001, China) for 30 min. The primary anti-CD11c antibody (Servicebio, 60258-1-Ig, China) was added and incubated overnight at 4 °C. Subsequently, the secondary antibody (Servicebio, GB23301, China) was added and incubated at 37 °C for 50 min. The slices were then immersed in diaminobenzidine liquid (Servicebio, G1211, China) for color development and rinsed with distilled water. Hematoxylin was used for counterstaining for 3 min before dehydrating and sealing the film. CD11c⁺ is a marker for detecting immature dendritic cells. The area density of the slices, indicative of immature dendritic cell expression, was quantitatively assessed utilizing Image-Pro Plus 6.0 software. For each group, images were captured by randomly selecting three fields of view at 200× magnification for each slice. The number of positive cells was determined based on the presence of the same brown-yellow color, ensuring consistent background light across all images.

2.5. Enzyme-linked immunosorbent assay (ELISA)

According to the instructions of the ELISA kit (K21013559, Huamei Company, China), we measured the expression levels of secretory immunoglobulin A (s-IgA) in rat lung and intestine tissues. We collected 100 mg of lung tissue and colon tissue each, homogenized them with a tissue grinder at −20 °C overnight, and then centrifuged them at 4 °C

for 5 min. Gradually, we added reagents to the supernatant and incubated it at 37 °C for 30 min. Finally, we measured the optical density at a wavelength of 450 nm using a microplate reader.

2.6. RNA extraction and real-time reverse transcription-polymerase chain reaction (RT-PCR) assay

To extract total RNA from 100 mg of rat lung tissue, RNAiso Plus (Invitrogen, Carlsbad, CA), chloroform, isopropanol, and ethanol were added sequentially. The PrimeScript™ RT Reagent Kit with gDNA Eraser (Perfect Real Time) kit (Takara, Dalian, China) was used according to the instructions to obtain cDNA. Real-time PCR analysis was conducted using the ABI 7500 Real-Time Quantitative PCR Detection System (Applied Biosystems, Darmstadt, Germany) with SYBR Premix Ex Taq II (Takara, Dalian, China) as the detection reagent. The primers used for RT-PCR can be found in Table 1.

2.7. 16S rRNA gene sequencing

Microbial DNA was extracted from rat stool samples using the QIAamp Fast DNA Stool Mini Kit (Cat: 51604) following the manufacturer's instructions. The final DNA concentration and purification were determined using the NanoDrop 2000 ultraviolet-visible spectrophotometer (Thermo Scientific, Wilmington, USA). The quality of the DNA was assessed using 1% agarose gel electrophoresis. The V3-V4 hypervariable regions of the bacterial 16S rRNA gene were amplified using the forward primer (5'-CCTACGGGSGCAGCAG-3') and the reverse primer (5'-GGACTACVVG GTATCTAA-TC-3') with a thermocycler PCR system (GeneAmp 9700, ABI, USA). The PCR reactions were performed with the following protocol: 3 min of denaturation at 95 °C, 20 s of denaturation at 98 °C, 15 s of annealing at 58 °C, and 20 s of extension at 72 °C, for 30 cycles. The temperature was then maintained at 72 °C for 5 min. The PCR reaction mixture contained 4 µL of

Table 1. Primer information.

mRNA	Forward Primer (5' → 3')	Reverse Primer (5' → 3')
IL-8	GCTGTGGCTCTCTTGGAACC	ATGCACTGGCATCGAAGCTCTG
TNF-α	GTCTAGCAAACCAACG	GAAGAGAACCTGGGAGTAGATAAGG
IL-17	CTGTTGCTGCTACTGAACCTGGAG	CCTCGGCGTTTGGACACACTG
IL-1β	TGTTTCCCTCCCTGCCTTGAC	CGACAATGCTGCCTCGTGACC
IL-18	CGACCGAACAGCCAACGAATCC	TCACAGATAGGGTCACAGCCAGTC
IL-10	CTGCTCTTACTGGCTGGAGTGAAG	TGGGTCTGGCTGACTGGGAAG
IL-6	CTGCAAGAGACTTCCATCCAG	AGTGGTATAGACAGGTCTGTTGG
IL-4	CAAGGAACACCACGGAGAACGAG	CTTCAAGCACGGTACATCACG
β-actin	GGAGAAGATTGTCACACAC	GGAGAAGATTGTCACACAC

5× FastPfu buffer, 2 µL of 2.5 mM dNTP, 0.8 µL of each primer (5 µM), 10 ng of template DNA, and 0.4 µL of FastPfu polymerase. The PCR product underwent purification via a 2% agarose gel and was subsequently quantified utilizing the Quanti-Fluor™-ST system (Promega, USA), following the manufacturer's guidelines. Paired-end sequencing was conducted employing the HiSeq platform with the PE250 strategy (Illumina, Inc., CA, USA). The long reads in the hypervariable area were spliced based on their overlapping relation. The 16S sequence was controlled to be between 220 bp and 500 bp and was further analyzed by compiling the data.

2.8. Detection of SCFAs in rat feces by gas chromatography-mass spectrometry (GC-MS)

After combining 0.05 – 0.1 g of the sample with 2 mL of a 10% phosphoric acid aqueous solution, the resulting mixture was vortexed for 2 min. Then, it was mixed with 1 mL of ether for 10 min and centrifuged at a low temperature for 20 min (4000 rpm). After that, 1 mL of ether was added and the mixture was centrifuged again (4000 rpm). The two extracts were combined and evaporated to yield 1 mL. Subsequently, ether was added to make a total volume of 2 mL. The content of relevant indicators was further analyzed following the instructions provided by the manufacturer.

2.9. Statistical analysis

All studies were designed to generate groups of equal size, using randomization and blinded analysis. The number of independent values is provided in the figure legends (biological replicates, not technical replicates), and statistical analysis was conducted using these independent values. All bar graphs in this study were generated using Graph-Pad Prism 9.0. One-way ANOVA with Tukey's HSD post hoc test was performed for the statistical analysis. The significance standard was set as $^{*}/^{#}P < 0.05$ and $^{**}/^{##}P < 0.01$. The 16S rRNA gene sequence analysis was performed using the QIIME and R software packages.

3. Results

3.1. Screening the active components of YQXF with ultra-high performance liquid chromatography-quadrupole time-of-flight (UHPLC-QTOF-MS)

UHPLC-QTOF-MS analysis was conducted to identify the active compounds in YQXF that

interacted with ECs. The fingerprint of YQXF showed a total of 45 distinct peaks (Fig. 1A and B). Further comparison with standard products revealed the presence of six types of compounds, namely amino acids, saponins, oligosaccharides, organic acids, adenosine, and esters (Table 2). These findings suggest that the active compounds in YQXF are complex mixtures composed of multiple substances.

3.2. YQXF inhibits inflammation in COPD rats

Tracheotomy with the infusion of LPS and cigarette smoke exposure is a recognized method for constructing an animal model of COPD [19]. In this experiment, the modeling cycle lasted for 84 days (Fig. 2A). Throughout this process, the model group experienced a significant decrease in survival rate and body weight. However, after administering YQXF, we observed a delay in the decline of both the survival rate and body weights (Fig. 2B and C). HE staining of lung tissue demonstrated that YQXF administration resulted in a dose-dependent reduction in inflammatory cell infiltration surrounding the airway, as compared to the model group (Fig. 2D). To further confirm the anti-inflammatory effect of YQXF, we analyzed the levels of pro-inflammatory and anti-inflammatory cytokines in lung tissue. Our findings indicate that YQXF reduced the levels of IL-8, TNF- α , IL-6, IL-18, IL-1 β , and IL-17, while increasing the levels of IL-4 and IL-10 (Fig. 2E).

3.3. YQXF improves immune function in COPD rats

The thymus and spleen are recognized as the primary immune organs. Thymus atrophy and spleen atrophy have been found to be positively associated with a decline in immune function. To investigate the impact of COPD model building on immune function, we measured the thymus index and spleen index. Compared to the control group, the model group exhibited a significant decrease in both thymus and spleen indexes ($P < 0.05$). YQXF group significantly increased relative to model group. However, spleen index was no significant changes were observed in each YQXF low dose group (Fig. 3A and B). Additionally, we examined s-IgA, a mucosal immunoglobulin involved in humoral immunity, and noticed an increase in its expression level in the lungs after YQXF administration (Fig. 3C). Previous studies have reported the accumulation of dendritic cells in COPD patients [35]. To identify these cells, we labeled them using the CD11c antibody. The results revealed an

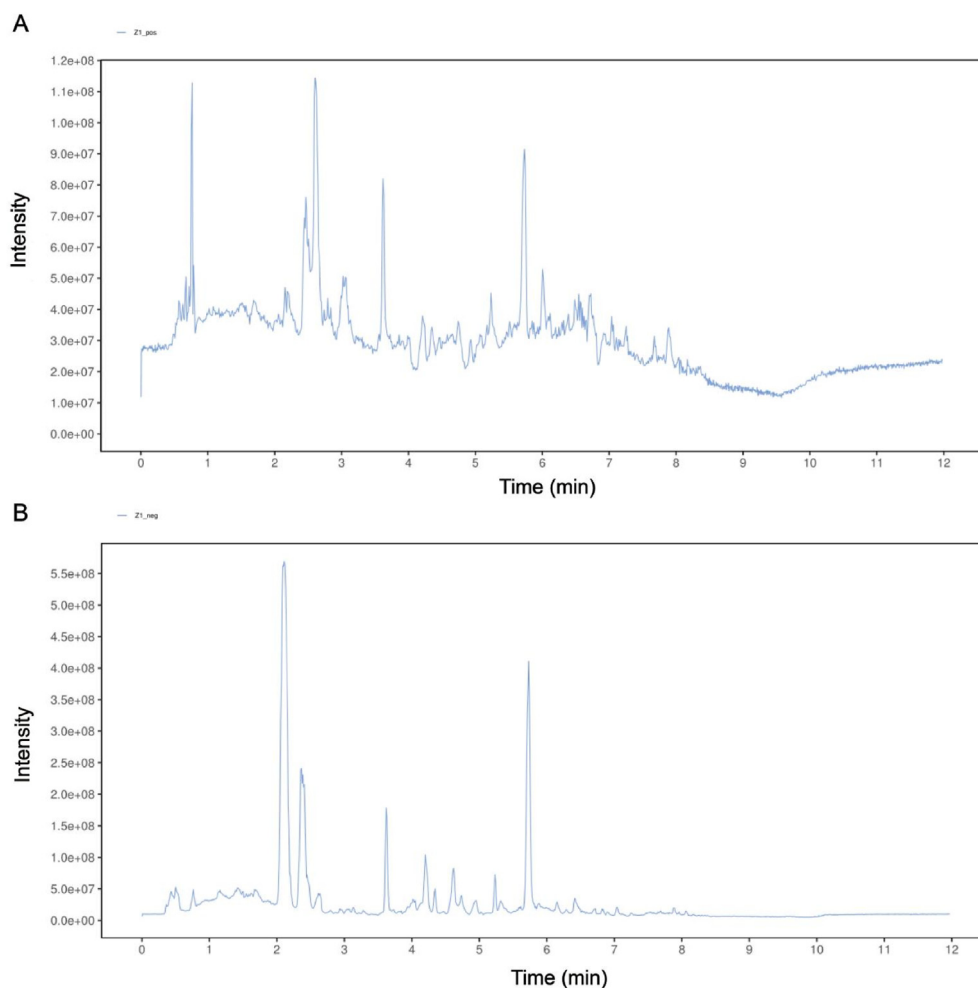


Fig. 1. (A) UHPLC-QTOF-MS analysis base peak intensity chromatograms of YQXF in positive mode. (B) UHPLC-QTOF-MS analysis base peak intensity chromatograms of YQXF in negative mode.

Table 2. Screening active components of YDP with UHPLC-QTOF-MS.

MS2 name	MS2 score	Electric	mzmed	rtmed	Peak area
Sinigrin	0.9576	-H	358.0254602	143.117	259224294.7
Sucrose	0.989	-H	341.1069819	343.825	166043602.8
D-Sorbitol	0.9823	-H	181.0693157	276.339	24856582.33
Sucrose	0.9632	+H	360.1452721	344.026	23848159.43
Citrate	0.9648	-H	191.0174767	452.298	23260354.72
Glycerophosphocholine	0.9888	+H	258.1051433	360.955	22862502.18
L-Malic acid	0.8985	-H	133.0121734	386.592	17996495.68
L-Proline	0.9994	-H	114.0542221	285.588	7422874.67
L-Canavanine	0.993	+H	177.0938728	367.684	5747351.35
Galactonic acid	0.9949	-H	195.0485555	363.4785	4338728.531
S-Methyl-5'-thiadenosine	0.9995	+H	298.0917921	90.522	4163917.933
Ononin	0.9882	+H	431.1278094	89.832	3987551.122
Ginsenoside Re	0.9996	-H	1005.565633	253.94	3491098.938
L-Asparagine	0.971	-H	131.0444055	354.214	3065779.842
2'-O-methyladenosine	0.9994	+H	282.1138758	99.762	2591857.027
L-Arginine	0.9854	-H	173.1018041	482.676	2357177.118
Deoxyadenosine	0.9991	+H	252.1032278	131.96	2307917.294
Ginsenoside Rb1	0.9999	-H	1167.618803	314.556	2100108.596
Cytidine	0.9974	+H	487.1727229	220.504	934142.3805
Thiamine	0.9972	+H	265.1056668	318.977	585148.5967
6''-O-Acetylglucitin	0.9862	+H	489.1334652	50.685	527114.4277

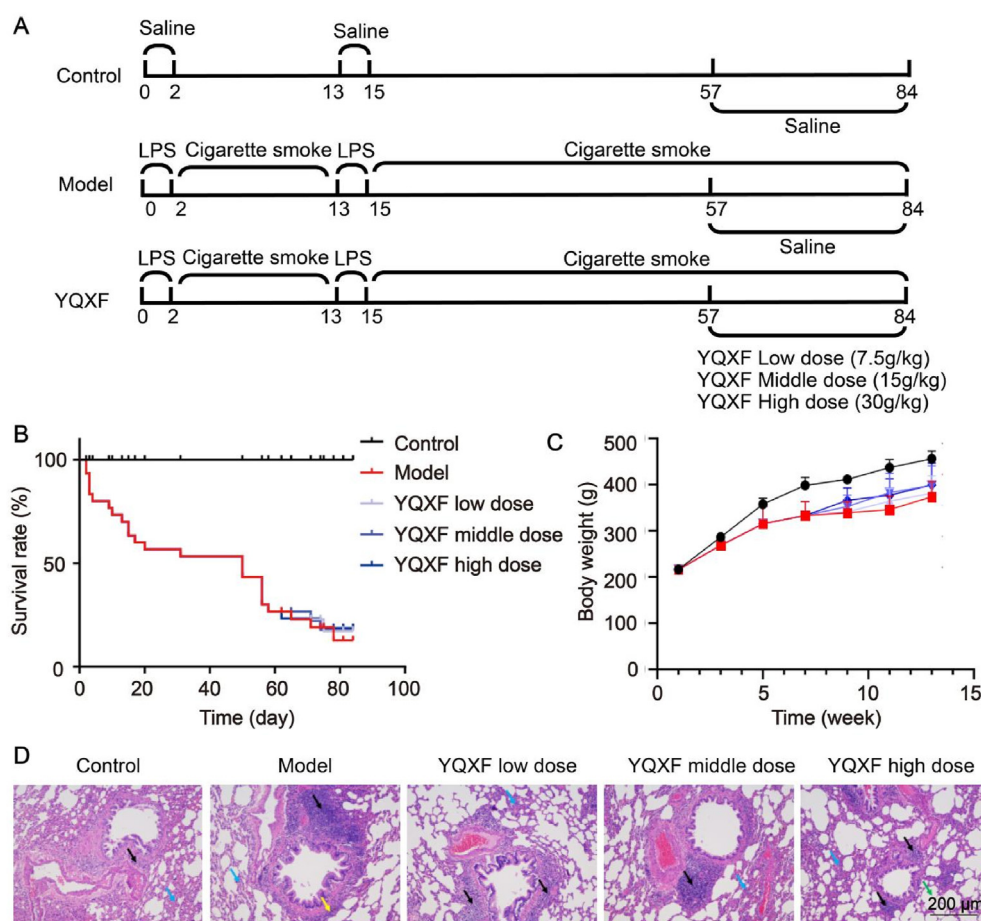


Fig. 2 (A) Experimental procedure schematic. (B) The survival rate of rats throughout the entire experimental period was recorded. (C) The body weight changes of the rats were recorded. (D) The levels of inflammation in the lung tissues of rats as reflected by HE staining ($\times 100$ magnification). (E) Relative mRNA expression level of IL-8, IL-18, IL-1 β , TNF- α , IL-6, IL-17, IL-10 and IL-4 in the rat lung tissues. Data shown are means \pm SEM of 4 independent experiments (* $P < 0.05$, ** $P < 0.01$, vs. control group; # $P < 0.05$, ### $P < 0.01$, vs. model group).

increase in the number of CD11c positive cells in the model group, while the number of positive cells in each YQXF dose group did not significantly differ from that in the control group (Fig. 3D). These findings suggest that YQXF intervention can effectively inhibit the loss of immune function in COPD models.

3.4. YQXF repairs the intestinal barrier in COPD rats

Clinical data reports that patients with COPD often exhibit impaired intestinal barrier function [36]. To investigate the potential repair effects of YQXF on the intestinal barrier, HE staining was performed on colon tissue. In the model group, we observed partial loss of the mucosal layer and muscle layer, as well as varying degrees of tissue edema. These findings support previous studies that suggest the formation of a COPD model can lead to intestinal damage [37]. Notably, when YQXF is

administered, damage to the mucosal and muscle layers is reduced, thereby protecting the physiological structure of the intestine (Fig. 4A). Additionally, we observed a decrease in intestinal s-IgA production in the model group. However, after YQXF intervention, the levels of s-IgA detected in each group exhibited an increase, which was found to be dose-dependent (Fig. 4B).

3.5. The effect of YQXF on remodeling the pulmonary microflora in COPD rats

Pulmonary microflora has been found to have the potential to predict the onset of respiratory diseases and may be affected by the establishment of the COPD model. In order to test this hypothesis, we conducted high-throughput sequencing of the 16S rRNA gene for pulmonary microflora. The results showed that the pulmonary microflora of the YQXF group underwent changes at various levels,

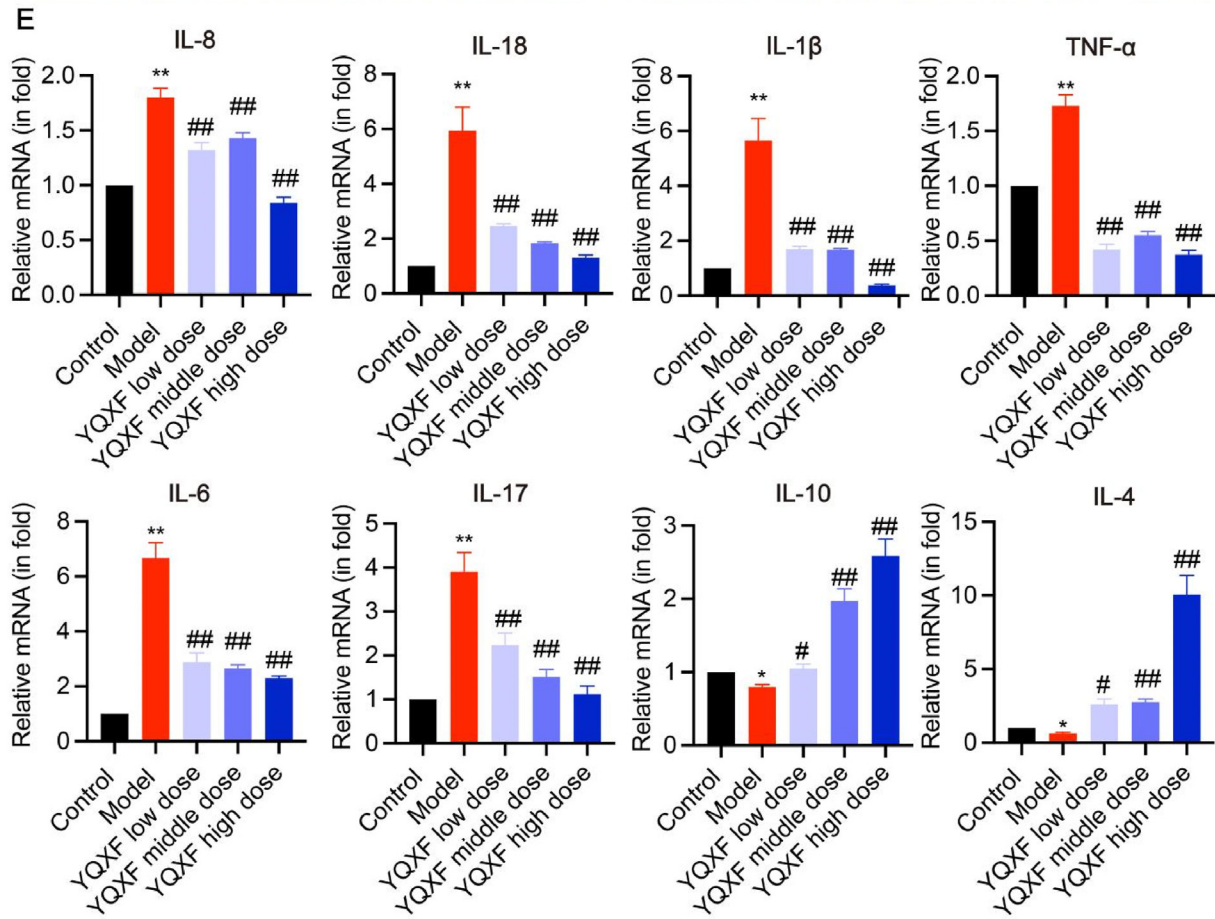


Fig. 2. (continued).

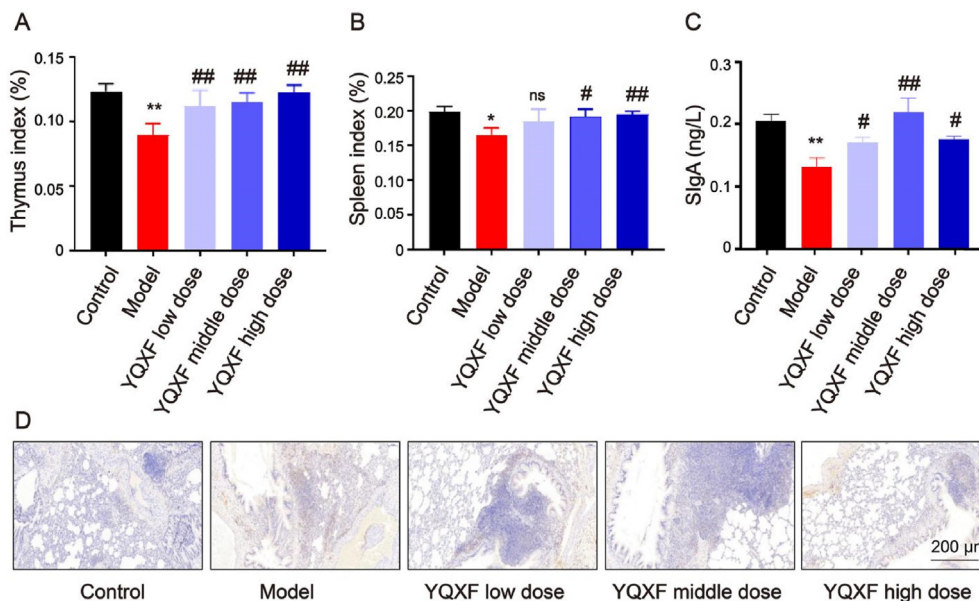


Fig. 3. (A) The thymus index in different groups. (B) The spleen index in different groups. (C) The relative content of sIgA in lung tissue was determined by ELISA. Data shown are means \pm SEM of 6 independent experiments (* P < 0.05, ** P < 0.01, vs. control group; # P < 0.05, ## P < 0.01, vs. model group; ns, non significant). (D) The number of immature dendritic cells in rat lung tissue was determined by immunohistochemistry. (\times 100 magnification).

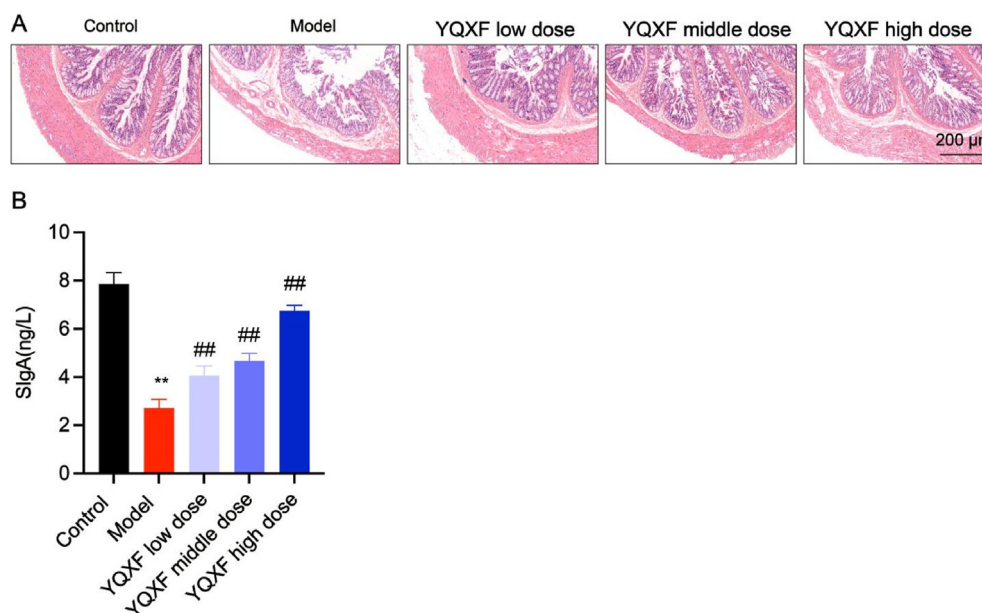


Fig. 4. (A) The levels of inflammation in the colon tissues of rats as reflected by HE staining ($\times 100$ magnification). (B) The relative content of sIgA in colon tissue was determined by ELISA. Data shown are means \pm SEM of 6 independent experiments (** $P < 0.01$, vs. control group; ## $P < 0.01$, vs. model group).

including phylum, class, order, family, and genus (Fig. 5A). The flower diagram of operational taxonomic units (OTU) reflected the number of common and specific OTUs in each group (Fig. 5B). Alpha diversity analysis provided insights into microbial diversity in each group, with the Chao 1 richness representing the relative richness of the microbial community. In terms of changes at the genus level, the Chao 1 richness decreased following YQXF intervention, indicating a reduction in the diversity of rat pulmonary microflora (Fig. 5C). To further validate these findings, we used beta diversity analysis to compare the differences between each group. The Analysis of Similarity (ANOSIM) was employed to compare differences both between and within groups. The Non-Metric Multi-dimensional Scaling illustrated the dissimilarities between each group, with the distance indicating the degree of similarity in microflora between groups. The composition within the same group exhibited higher similarity (Fig. 5D). The results demonstrated that the relative abundance of *Roseburia* (1.92%) significantly decreased in the model group ($P < 0.05$), but increased following YQXF intervention. The relative abundance of *Clostridium sensu stricto* (4.91%) increased in the model group ($P > 0.05$) but decreased following YQXF intervention. The most abundant bacteria were listed (Fig. 5E). The heatmap indicated the similarities and differences in pulmonary microflora composition of each group. The linear discriminant analysis (LDA)

effect size revealed the bacteria that had a significant impact on the sample division. The legend on the right side of the cluster tree displayed the names of the bacteria in English letters. The LDA score (LDA threshold 2) of the bacteria that had significant effects was obtained using LDA (Fig. 5F), and a Spearman correlation heatmap was drawn between horizontal bacteria using the Corrplot package of R software. Blue color represented a positive correlation, while red color represented a negative correlation. The darker the color, the stronger the correlation between bacteria groups (Fig. 5G). The analysis of the Spearman correlation heatmap between environmental factors and bacterial populations demonstrated the relationship between various indicators in this study and the relative abundance of the top 20 bacterial species (Fig. 5H). Generally, dysregulated pulmonary flora that causes COPD was remodeled by YQXF.

3.6. YQXF modulate intestinal microflora in rats

Previous experiments have confirmed that YQXF has the ability to repair the damaged intestinal barrier, which includes the microbial barrier. The intestinal flora plays a crucial role in regulating the immune system [38]. Immune tolerance establishment is a key factor in the regulation of the innate immune system, contributing to the development of intestinal mucosal immunity and the regulation of the human immune system. Clinical studies have

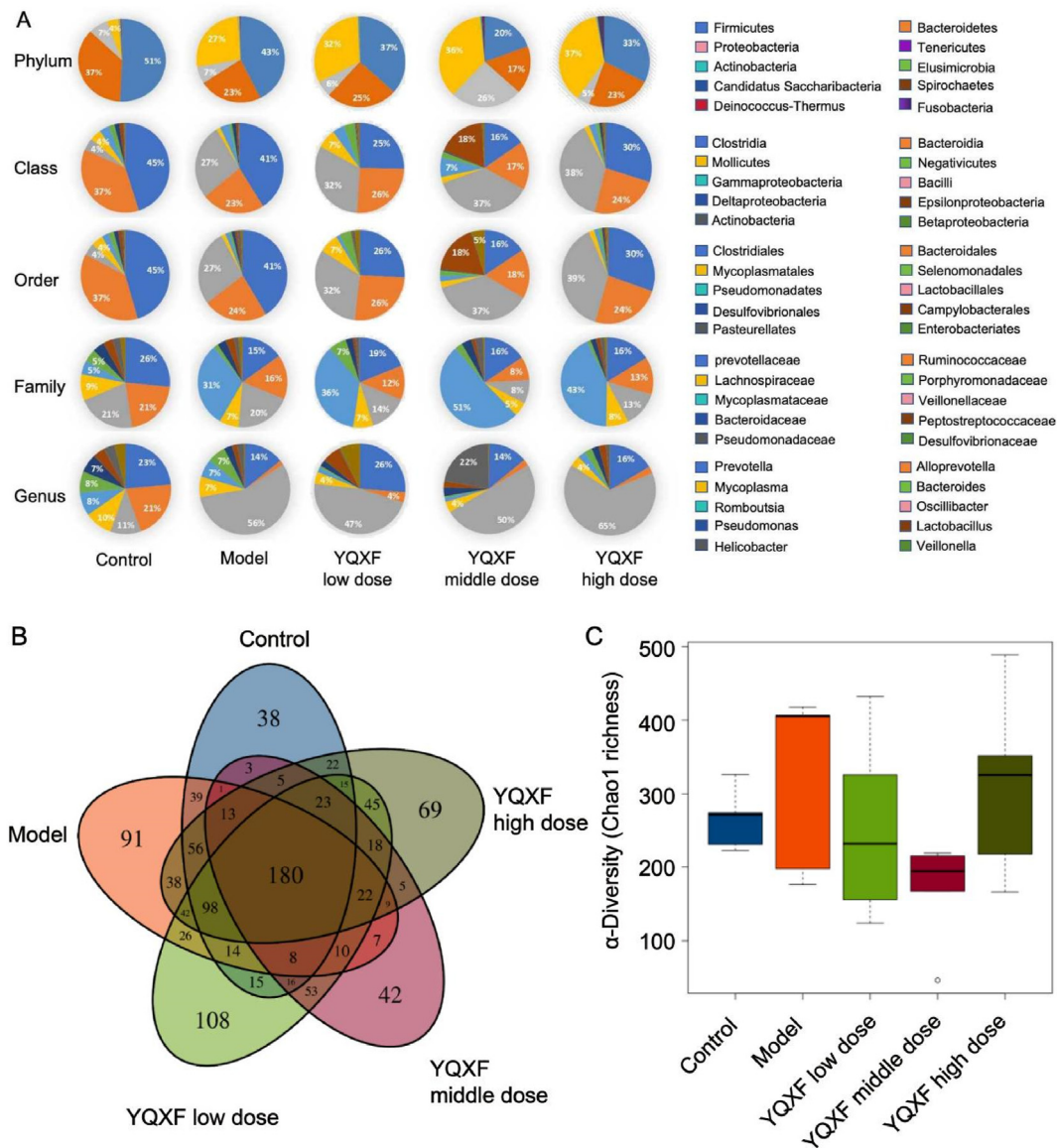


Fig. 5 (A) Relative abundance of phylum, class, order, family and genus levels in pulmonary flora of rats, top 26 taxa was shown. (B) Changes of rat pulmonary flora in OTU level. (C) Changes of Alpha diversity in rat pulmonary flora. (D) Changes of Beta diversity in rat pulmonary flora. (E) The relative changes of pulmonary flora at genus level. (F) Changes of rat pulmonary flora in LEfSe difference analysis was used to find the bacteria with significant differences among different groups. (G) Correlation analysis between bacteria and bacteria in genus level. (H) Correlation analysis between fungi and environmental factors in genus level.

reported that patients with chronic obstructive pulmonary disease experience impaired intestinal integrity due to intestinal mucosal ischemia and hypoxia resulting from increased metabolic demand. This can lead to an imbalance or migration of intestinal flora [39]. By analyzing the intestinal bacteria in each group, significant changes were observed in the phylum, class, order, family, and genus of the intestinal flora in the YQXF groups. In our study, we observed changes in the intestinal flora of each YQXF dose group at the phylum, class, order, family,

and genus levels (Fig. 6A), which aligns with previous reports. To assess the abundance and diversity of the microbiota, we employed the OTU clustering method, alpha diversity, and ANOSIM, which indicate the number of common and specific OTUs in each group. The OTU flower chart provides insights into the number of common and specific OTUs in each group YQXF treatment increased the diversity of intestinal flora and reduced its abundance in rats. The differences within the group were greater than those between groups ($R = 0.359$, $P = 0.001$).

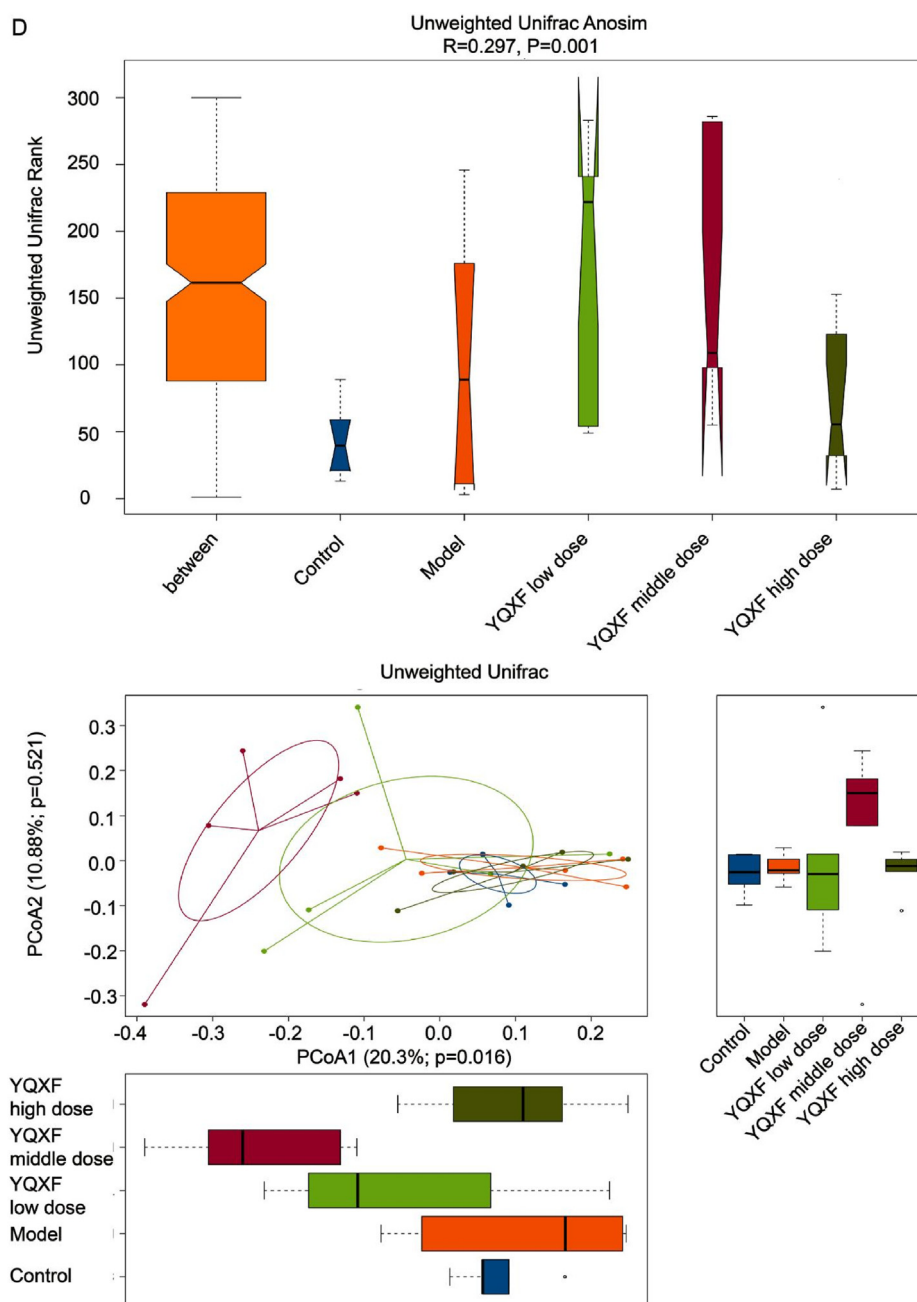


Fig. 5. (continued).

Composition within the group was more similar than that between groups. Compared to the blank group, the relative abundance of *Oscillibacter* (5.66%) in the model group decreased significantly ($P < 0.05$) and that of *Escherichia/Shigella* (4.42%) increased following drug intervention ($P < 0.05$), but decreased following drug intervention. The LDA score was obtained by the bacteria that had significant effects using LDA (Supplementary materials). We analyzed the correlation between bacteria, other indexes, and

bacteria at the genus level. The findings imply that YQXF has the potential to modulate the composition of gut microbiota.

3.7. YQXF promotes production of SCFAs by intestinal flora

Short-chain fatty acids (SCFAs), such as acetic acid, propionic acid, and butyric acid, are synthesized by colonic bacteria during the fermentation of

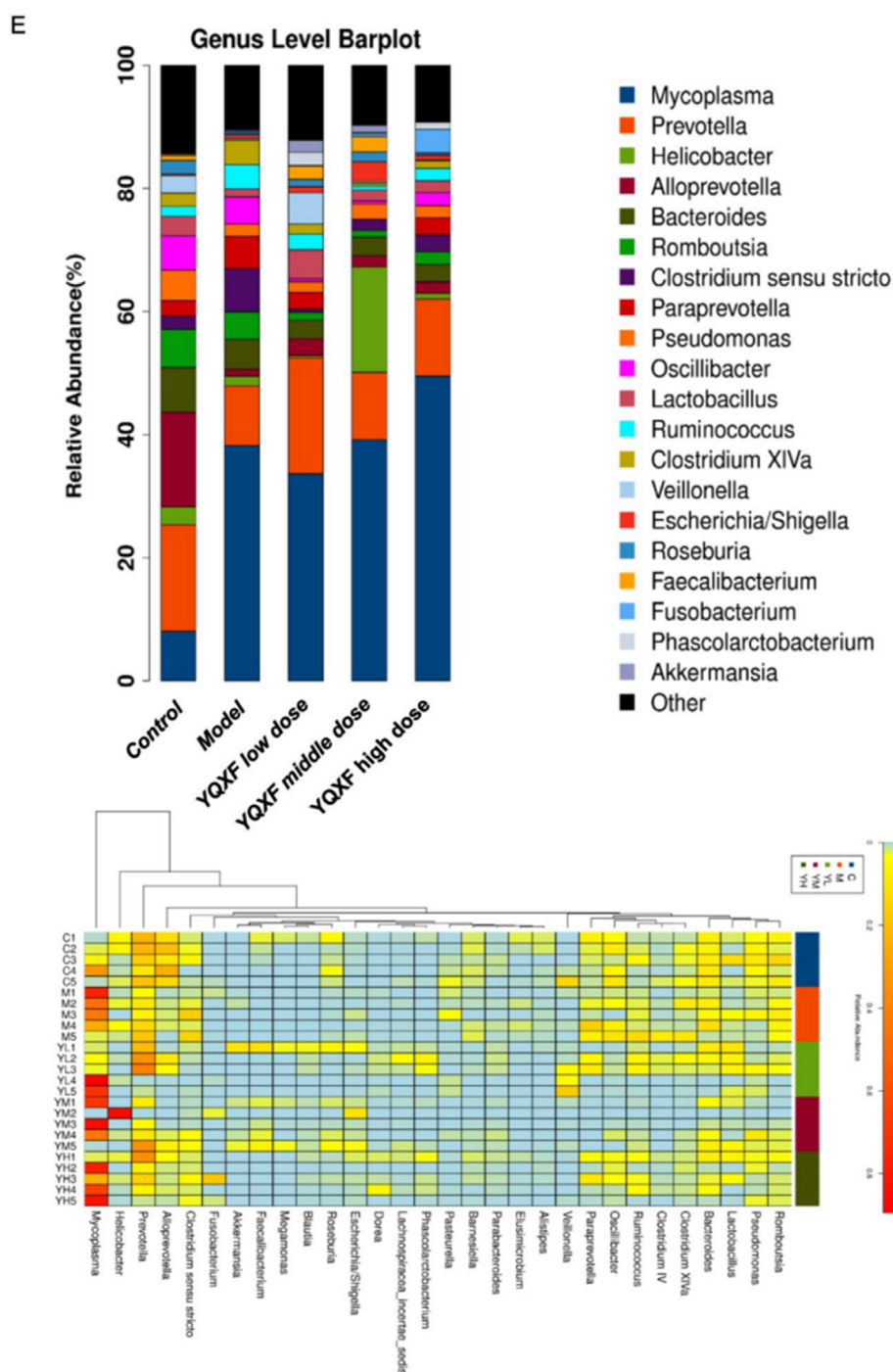


Fig. 5 (continued).

undigested food. These SCFAs provide energy for colonic cells and have been reported to possess strong immunomodulatory and anti-inflammatory properties [40]. Our measurements indicate that the levels of acetic acid, propionic acid, and butyric acid

were significantly lower in the model group compared to the control group ($P < 0.05$). However, the reduction of SCFAs was subsequently reversed following the administration of YQXF (Fig. 7A–C). These findings suggest that a disorder in SCFAs



Fig. 5 (continued).

metabolism may play a crucial role in the pathogenesis of COPD, and YQXF appears to alleviate COPD by regulating SCFAs metabolism.

3.8. YQXF is involved in microflora repair both pulmonary and pntestinal flora

16S rRNA sequencing identified 70 identical floral species out of a total of 162 species detected in the lungs and 84 species detected in the intestines (Fig. 8A). Notably, there was a marked decrease in the abundance of *Alloprevotella* spp. and *Roseburia* spp. in both the lungs and intestines of the model group ($P < 0.05$), while *Oscillibacter* spp. decreased only in the intestines ($P < 0.05$) (Fig. 8B and C).

YQXF, at medium or high doses, significantly increased the levels of *Alloprevotella* spp., *Roseburia* spp., and *Lactobacillus* spp. in the intestines ($P < 0.05$). Interestingly, *Oscillibacter* spp. showed a remarkable increase ($P < 0.05$) in both the lungs and intestines when low-dose YQXF was administered (Fig. 8B and C). The abundance of *Escherichia/Shigella* and *Clostridium sensu stricto* was elevated in the intestinal flora of the model group ($P < 0.05$). YQXF responded to the increased *Fusobacterium* and *Clostridium sensu stricto* in both the lungs and intestines ($P < 0.05$), but there was no reaction in either the lungs or intestines to *Escherichia/Shigella* (Fig. 8D and E). These results indicate that, although the species and location varied, there were changes in bacterial

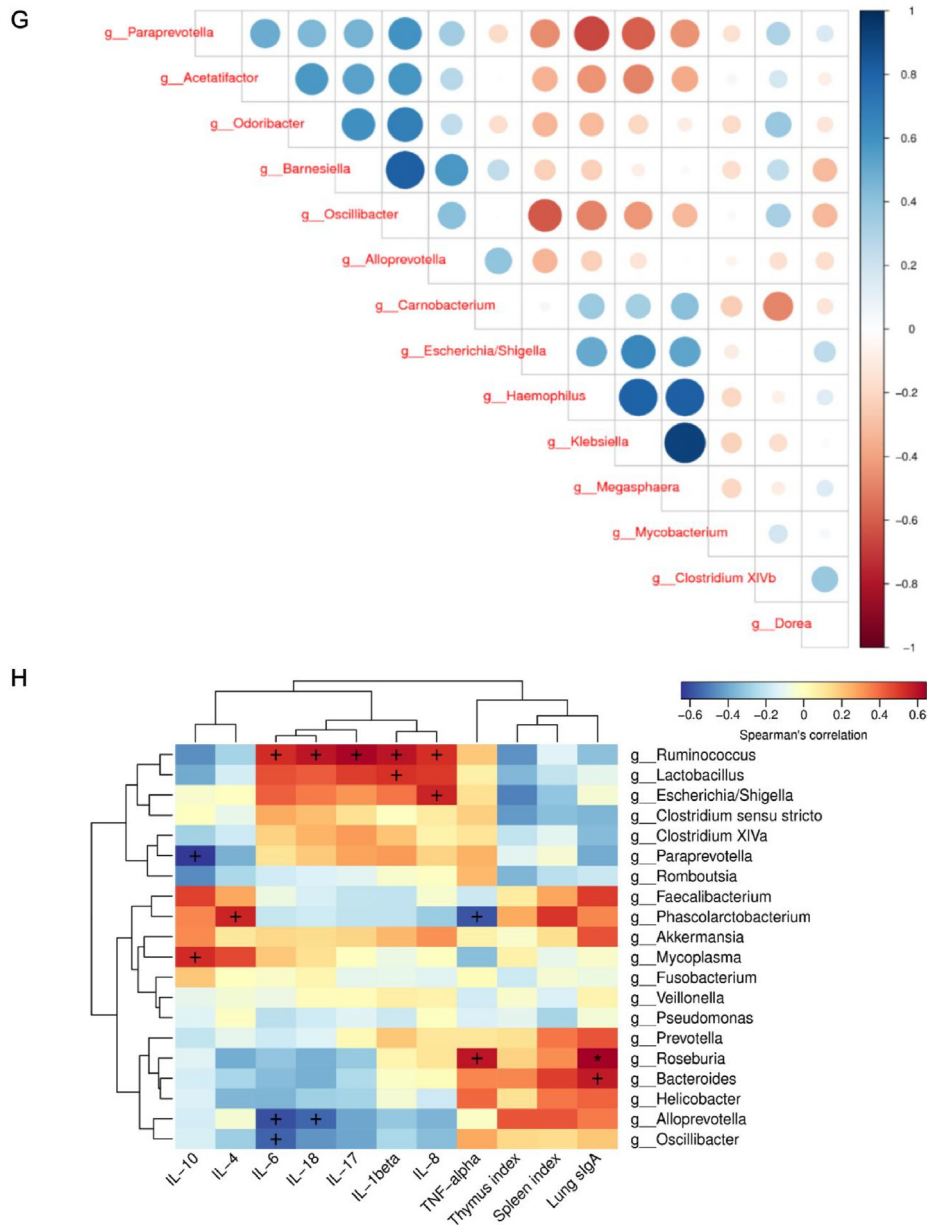


Fig. 5 (continued).

abundance in both the lungs and intestines during the establishment of the COPD model. YQXF partially restored bacterial abundance in the lungs and intestines.

4. Discussion

It was previously believed that the lungs were sterile, but recent discoveries have revealed the presence of a distinct microbiota within the lung

[41]. Furthermore, emerging evidence suggests that the lung microbiota can be influenced by signals from other parts of the body, including the intestine. This microbial composition plays a significant role in the development and progression of COPD [9]. Our study further supports this notion by demonstrating that the onset of COPD affects both the lung and gut, resulting in pathophysiological and microbiome alterations. These findings suggest that COPD should not be viewed solely as a local organ

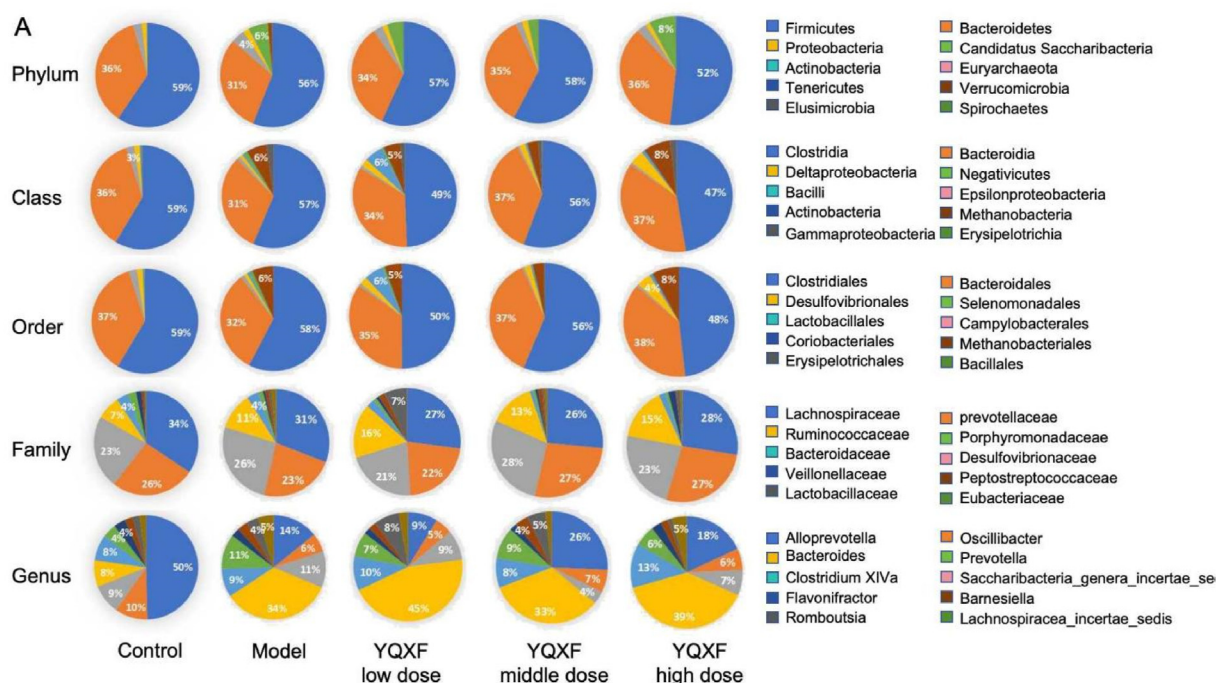


Fig. 6. (A) Relative abundance of phylum, class, order, family and genus levels in intestinal flora of rats, top 26 taxa was shown.

dysfunction but rather as a systemic disease. YQXF, a traditional Chinese herbal formula, has been extensively utilized in clinical settings for managing COPD. Notably, it exhibits promising effects in preserving the physiological structure of the lung and intestine, as well as restoring a healthy abundance of microbiota in the body. This study

emphasizes the potential of YQXF as a clinical adjuvant for COPD.

LPS combined with cigarette smoke induced COPD in rats, which is commonly used for pharmacological evaluation. In this study, COPD rats were successfully established. We observed exacerbated lung inflammation, decreased immune

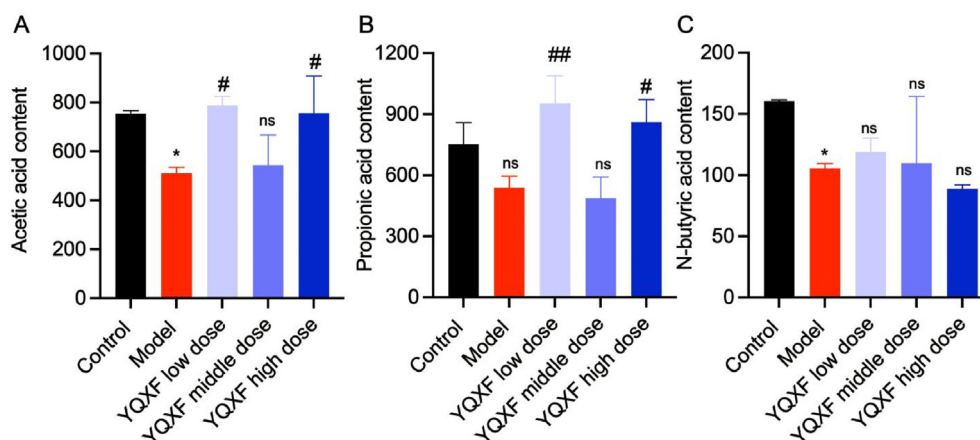


Fig. 7. (A) Changes of acetic acid content in intestinal contents. (B) Changes of propionic acid content in intestinal contents. (C) Changes of N-butyric acid content in intestinal contents (* $P < 0.05$, vs. control group; # $P < 0.05$, ## $P < 0.01$, vs. model group; ns, non significant).

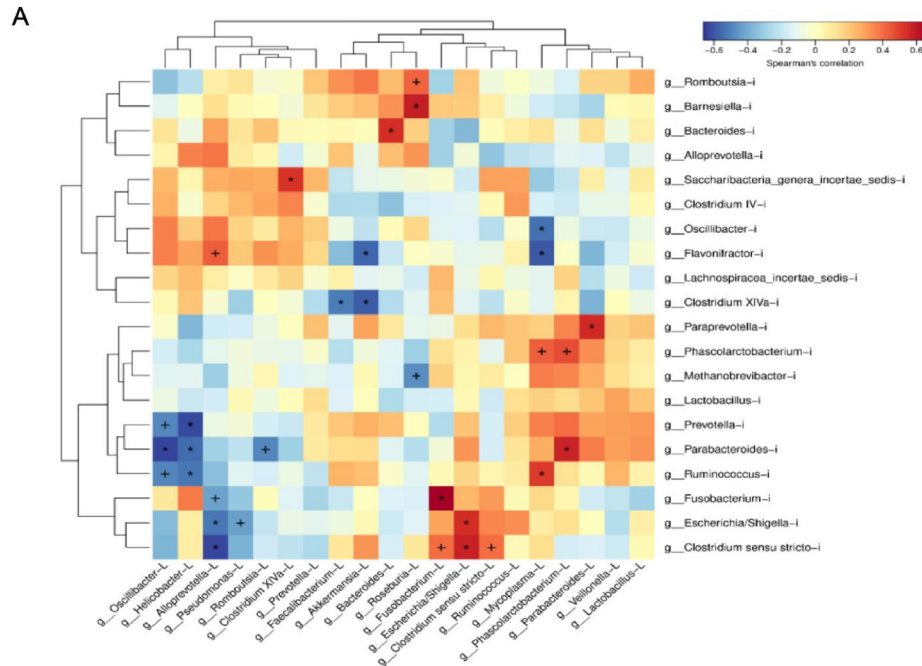


Fig. 8 (A) Correlation analysis of pulmonary flora and intestinal flora at genus level. (B,D) Changes of beneficial bacteria in pulmonary and intestinal flora. (C,E) Changes of harmful bacteria in pulmonary and intestinal flora (** $P < 0.01$, vs. control group; * $P < 0.05$, ## $P < 0.01$, vs. model group; ns, non significant).

function, and impaired intestinal barrier function in the model group of rats. Encouragingly, YQXF exhibited significant therapeutic effects in our study. The changes in microbial community structure and abundance were another aspect of this study that we focused on. Our data indicate a significant decrease in the levels of *Prevotella*, *Roseburia*, *Oscillibacter*, and *Lactobacillus* in the model group. Previous studies have reported that *Prevotella* mainly parasitizes the respiratory tract and is associated with the induction of chronic inflammation [42]. Although some studies suggest that high levels of *Prevotella* often appear in inflammatory diseases, we found lower levels of *Prevotella* compared to the control group, indicating that *Prevotella* may be at a competitive disadvantage. *Roseburia* is a bacterium that produces butyrate and has been shown to alleviate inflammation in mice. *Oscillibacter* secretes anti-inflammatory molecules and exhibits lower expression in COPD patients. *Lactobacillus* has been reported to be beneficial in alleviating COPD symptoms and also helps maintain immune function, protect gastric mucosa, and improve digestion and absorption [43]. Our study further confirms and refines the aforementioned hypotheses.

In addition, we also analyzed the bacterial species with increased expression in both lung and gut. In COPD rats, the levels of *Fusobacterium*, *Escherichia/Shigella*, and *Clostridium sensu stricto* were increased.

However, after YQXF treatment, the abundance of these bacteria decreased. Previous reports have shown that there is a significant difference between spore-forming *Fusobacterium* and normal bacteria in the bronchoalveolar lavage fluid of smokers and COPD patients [44]. This deviation can lead to epithelial cell damage and induce abnormal inflammation, which can disrupt the intestinal barrier. Furthermore, the prevalence of *Escherichia coli/Shigella* is elevated in individuals with inflammatory bowel disease, a condition thought to exacerbate inflammatory responses [45]. *Clostridium sensu stricto* is prone to producing toxins in the body, leading to infections and intestinal diseases [46].

As discovered by other researchers, the majority of microbial communities initially colonize the oral-pharyngeal region, with some entering the gastrointestinal tract through food ingestion and others entering the respiratory tract through inhalation [47]. These two organs also exhibit similarities in terms of tissue cells and immune effector molecules. For instance, both the lungs and the gut contain goblet cells and s-IgA, indicating that they provide favorable environments for microbial communities. Rats with intestinal diseases also show synchronized changes in respiratory and intestinal microbial communities, suggesting a potential collaborative

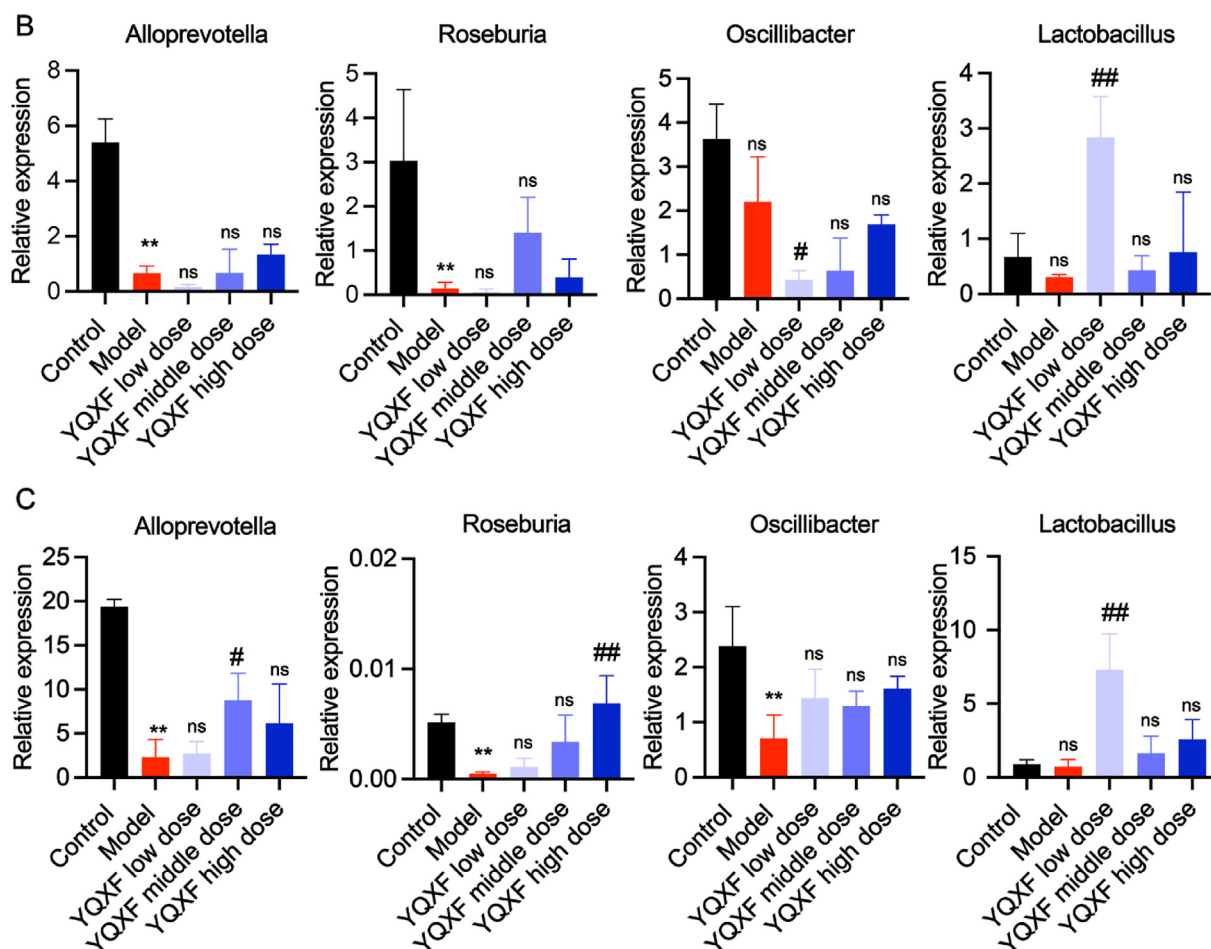


Fig. 8. (continued).

interaction to maintain gut health. Furthermore, patients with inflammatory bowel disease have a relatively higher risk of developing respiratory system diseases such as COPD [48], and irritable bowel syndrome is a risk factor for COPD exacerbation [49]. Our study further supports the notion that there is partial overlap in the bacterial species colonizing the lungs and the gut. Therefore, we believe that microbial communities influence host immunity through the release of metabolites, proteins, and chemical substances, thereby supporting the overall health of the lungs and the gut.

However, our study has limitations. First, although we observed changes in metabolites such as SCFAs additional experiments are needed to validate their precise impact on the disease. Second,

while we have provided preliminary evidence of YQXF's protective effects on immune function in COPD models, we have not extensively explored its specific regulatory mechanisms. Further experimentation is necessary to comprehensively elucidate the scientific significance of YQXF's multi-target effects in the prevention and treatment of COPD, thereby providing valuable insights for its clinical application.

In conclusion, our research suggests that YQXF can alleviate COPD by mitigating inflammation, modulating immunity, repairing damaged intestinal barriers, and restoring the balance of lung and gut microbiota. Therefore, YQXF holds potential as a complementary drug to enhance patients' quality of life and minimize drug side effects.

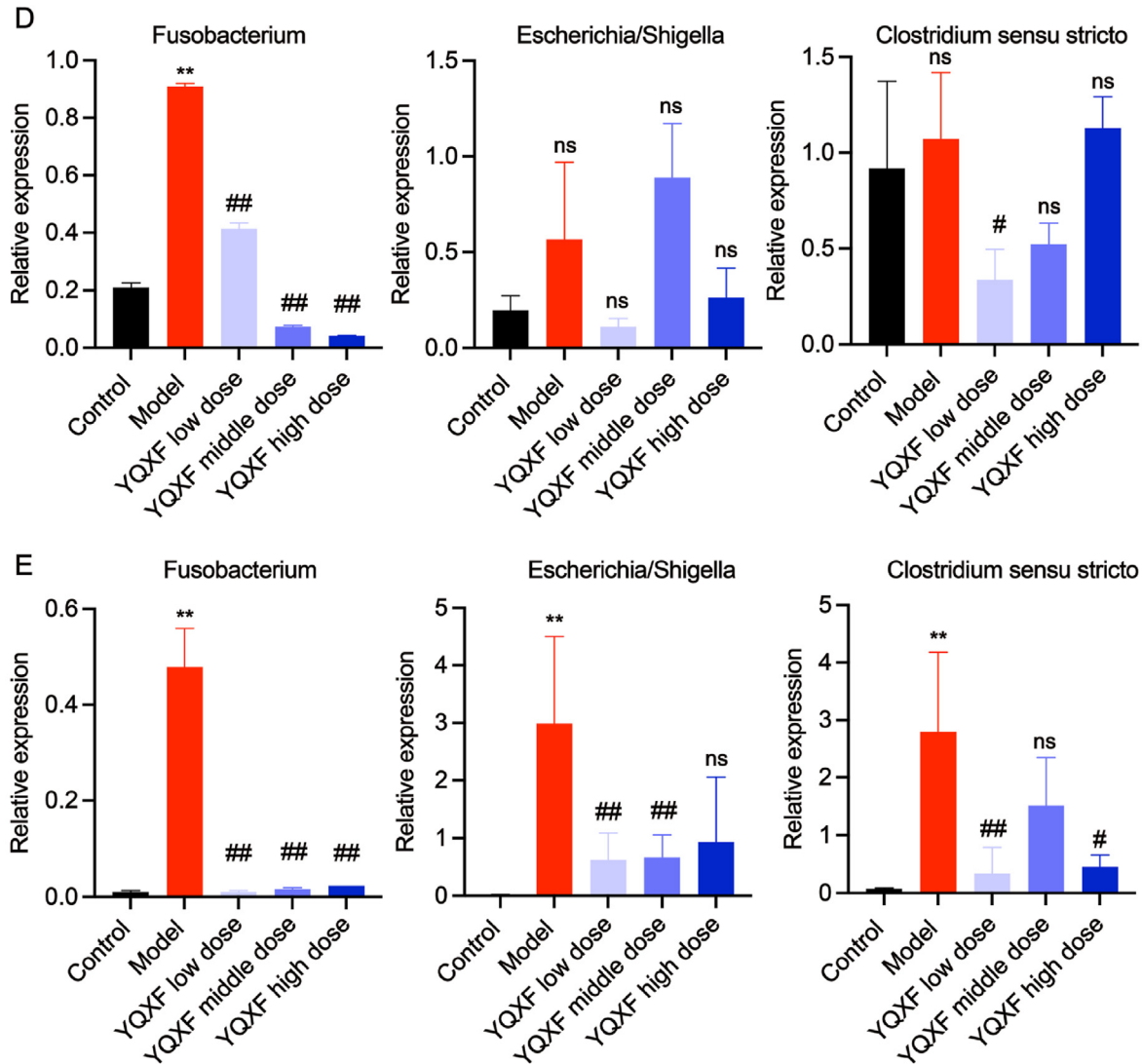


Fig. 8 (continued).

Ethics approval and consent to participate

The animal research protocol was approved by the Institutional Review Committee of Animal Experiment Ethics of Yunnan University of Traditional Chinese Medicine. The approval number assigned to the protocol is R-06202023. The protocol was approved on June 18, 2020.

Author contributions

Zhong-Shan Yang contributed to the conceptualization, methodology, supervision, and writing—original draft. Si-Si Han, Li-Yun Song, and Peng-Tao Liang contributed to animal experiments and investigations. Yin-Ying Wang, Yi Ying, and Li Li contributed to the writing—review and editing. Jia-Li Yuan contributed to the conceptualization, methodology, and editing.

Data availability statement

The data that support the findings of this study are available from the corresponding authors upon reasonable request.

Conflicts of interest

The authors declare no conflict of interest.

Acknowledgments

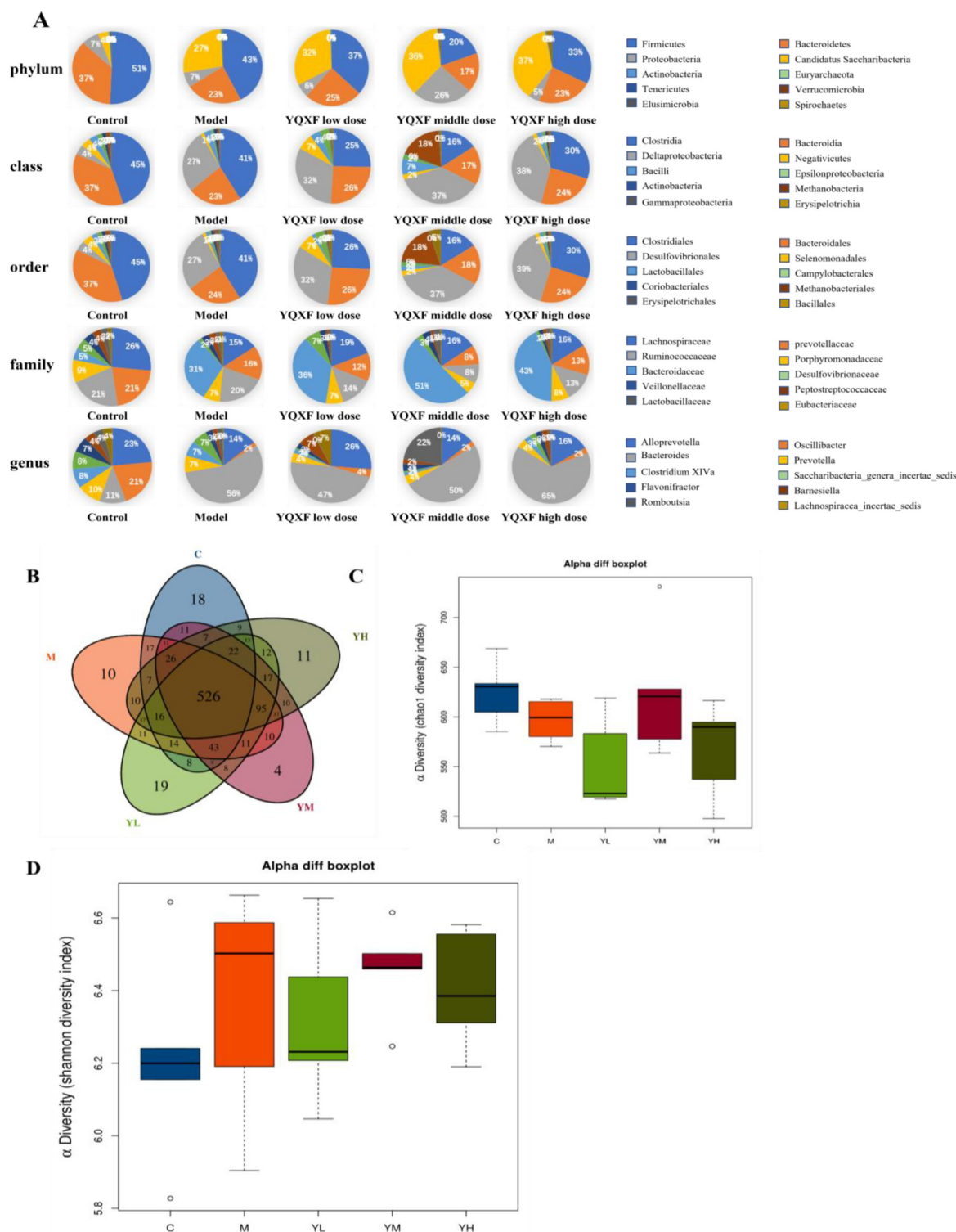
This work was funded in part by a grant from the National Natural Science Foundation of China (82360017), a grant from Yunnan Provincial Science and Technology Department (202005AC-160058, 202201AS070084, 202101AZ070001-012, 202307AB110046, YNWR-QNBJ-2019-069). Central government's fund for guiding local science and

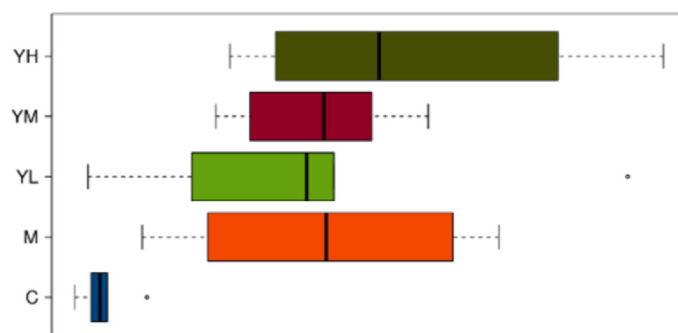
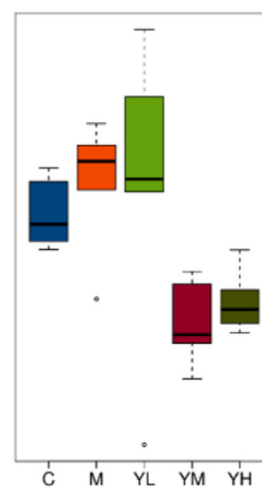
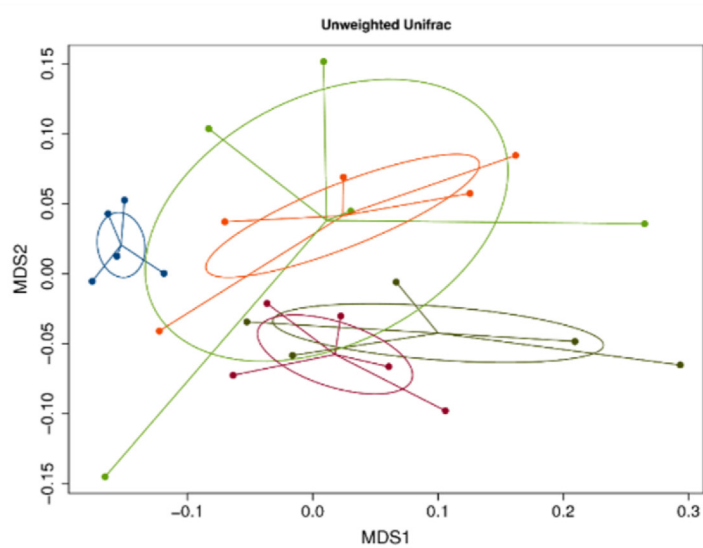
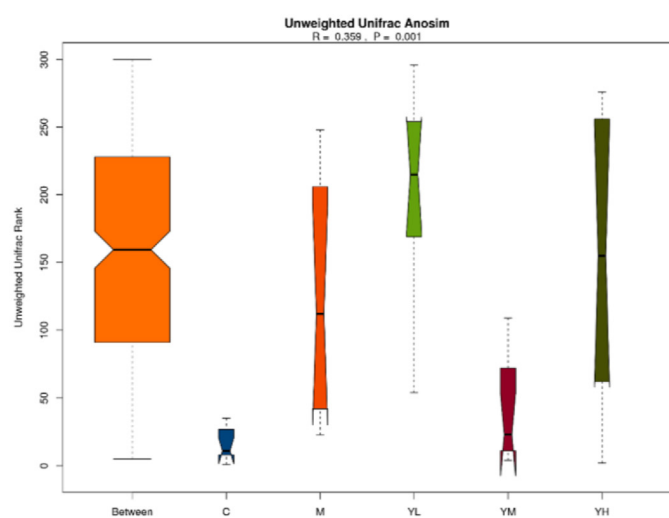
technology development. Chen Xiaofeng's contribution to the language editing of the article.

Supplementary materials

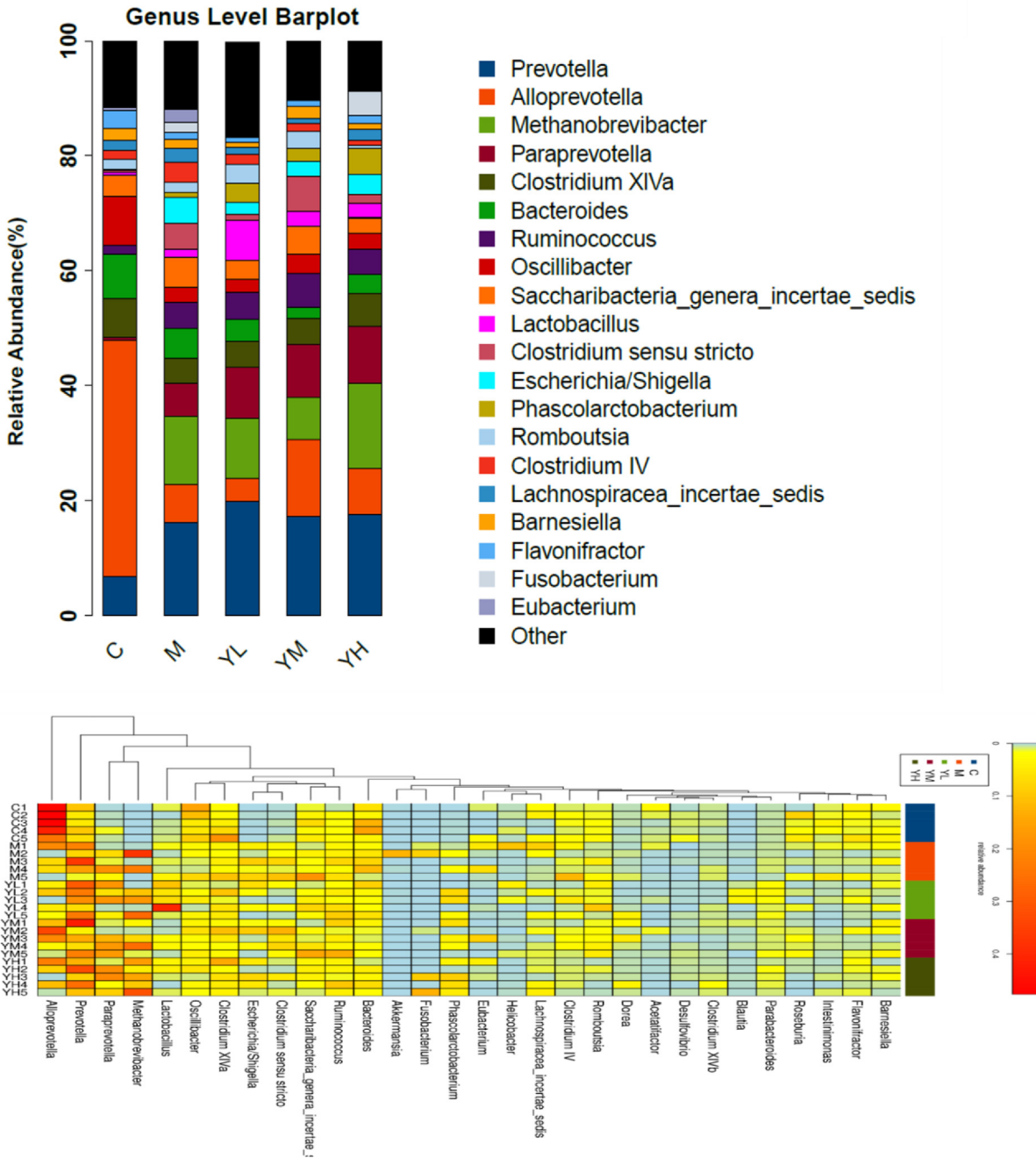
Supplementary Figure: (A) Relative abundance of phylum, class, order, family and genus levels in intestinal flora of rats, top 26 taxa was shown. (B) Changes of rat intestinal flora in OTU level. (C) Changes of Alpha diversity in rat intestinal flora. (D)

Changes of Beta diversity in rat intestinal flora. (E) The relative changes of intestinal flora at genus level. (F) Changes of rat intestinal flora in LEfSe difference analysis was used to find the bacteria with significant differences among different groups. (G) Correlation analysis between bacteria and bacteria in genus level. (H) Correlation analysis between fungi and environmental factors in genus level. (I) Correlation analysis of gut microbiota and environmental factors.

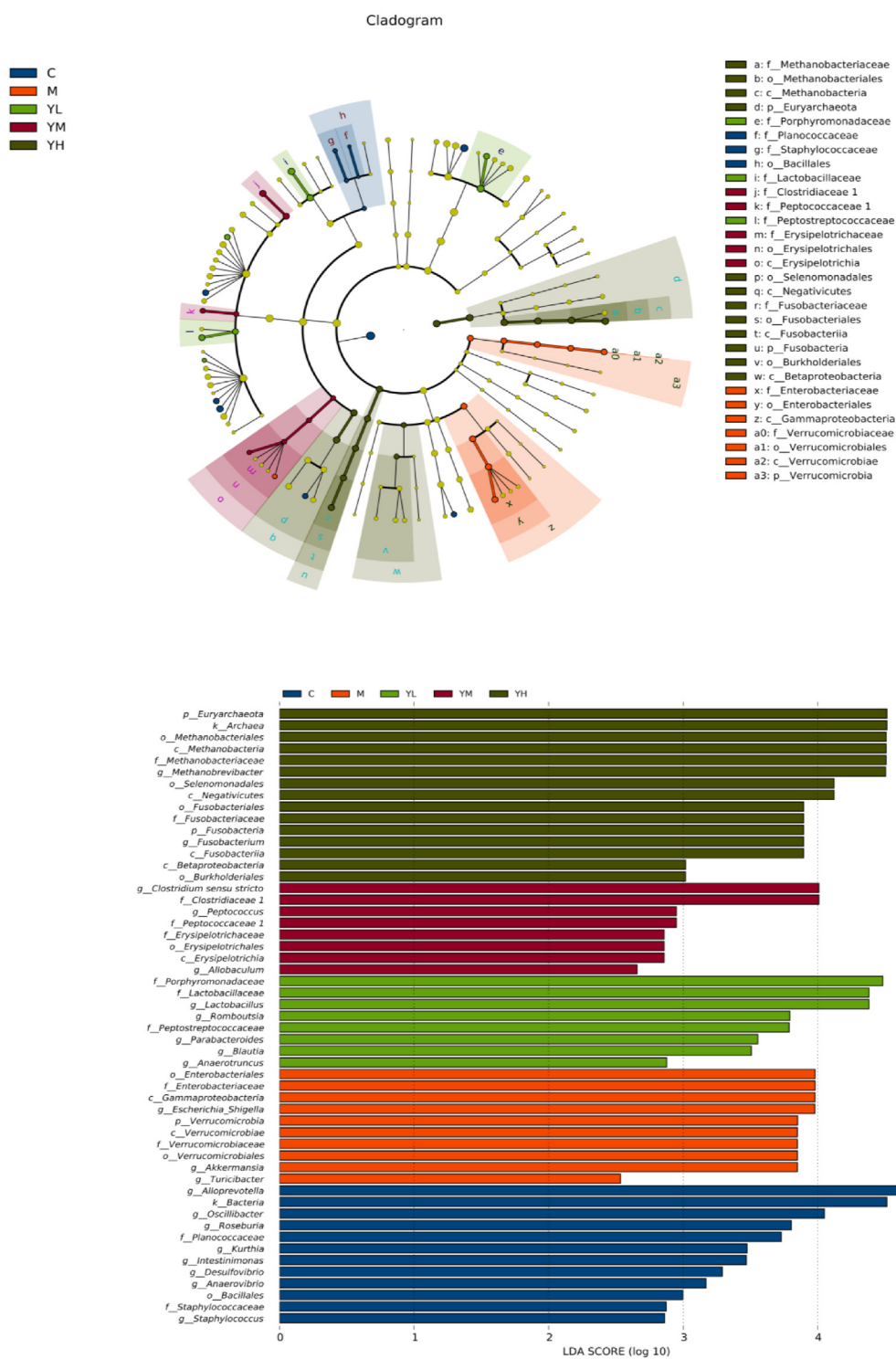


E

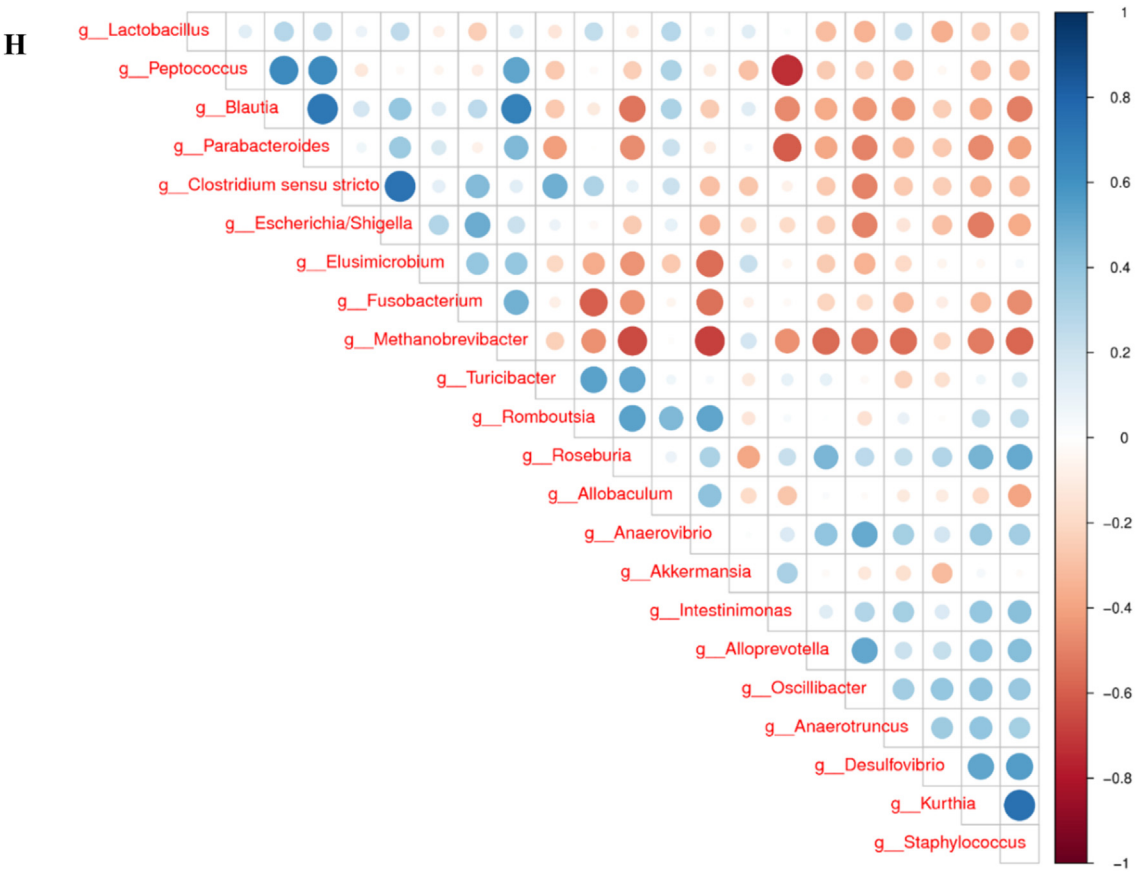
F



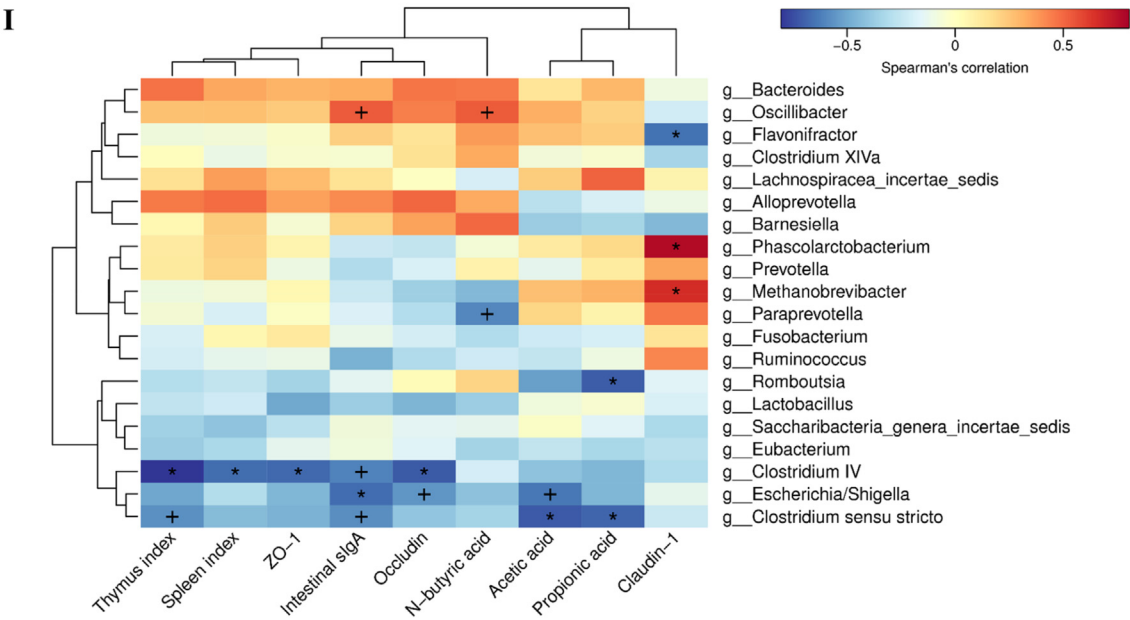
G



Correlation analysis between pulmonary microbiota and bacterial genera



Correlation analysis between lung microbiota and environmental factors



References

- [1] Iliaz S, Tanriverdio E, Chousein EGU, Ozturk S, Iliaz R, Cetinkaya E, et al. Importance of pulmonary artery to ascending aorta ratio in chronic obstructive pulmonary disease. *Clin Respir J* 2018;12:961–5. <https://doi.org/10.1111/crj.12612>.
- [2] Katsiki N, Steiropoulos P, Papanas N, Mikhailidis DP. Diabetes mellitus and chronic obstructive pulmonary disease: an overview. *Exp Clin Endocrinol Diabetes* 2021;129:699–704. <https://doi.org/10.1055/a-1038-3883>.
- [3] Lee KC, Wu YT, Chien WC, Chung CH, Shen CH, Chen LC, et al. Osteoporosis and the risk of temporomandibular disorder in chronic obstructive pulmonary disease. *J Bone Miner Metabol* 2021;39:201–11. <https://doi.org/10.1007/s00774-020-01134-w>.
- [4] Ivziku D, Clari M, Piredda M, De Marinis MG, Matarese M. Anxiety, depression and quality of life in chronic obstructive pulmonary disease patients and caregivers: an actor-partner interdependence model analysis. *Qual Life Res* 2019;28:461–72. <https://doi.org/10.1007/s11136-018-2024-z>.
- [5] Gómez FP, Rodríguez-Roisin R. Global initiative for chronic obstructive lung disease (GOLD) guidelines for chronic obstructive pulmonary disease. *Curr Opin Pulm Med* 2002;8:81–6. <https://doi.org/10.1097/00063198-200203000-00001>.
- [6] Morris DJ, Brem AS. Role of gut metabolism of adrenal corticosteroids and hypertension: clues gut-cleansing antibiotics give us. *Physiol Genomics* 2019;51:83–9. <https://doi.org/10.1152/physiolgenomics.00115.2018>.
- [7] Zhu HZ, Liang YD, Ma QY, Hao WZ, Li XJ, Wu MS, et al. Xiaoyaosan improves depressive-like behavior in rats with chronic immobilization stress through modulation of the gut microbiota. *Biomed Pharmacother* 2019;112:108621. <https://doi.org/10.1016/j.biopha.2019.108621>.
- [8] Chauhan A, Kumar R, Sharma S, Mahanta M, Vayuruu SK, Nayak B, et al. Fecal microbiota transplantation in hepatitis B e antigen-positive chronic hepatitis B patients: a pilot study. *Dig Dis Sci* 2021;66:873–80. <https://doi.org/10.1007/s10620-020-06246-x>.
- [9] Shi CY, Yu CH, Yu WY, Ying HZ. Gut-lung microbiota in chronic pulmonary diseases: evolution, pathogenesis, and therapeutics. *Can J Infect Dis Med Microbiol* 2021;2021:9278441. <https://doi.org/10.1155/2021/9278441>.
- [10] Gao J, Chen H, Xu L, Li S, Yan H, Jiang L, et al. Effects of intestinal microorganisms on influenza-infected mice with antibiotic-induced intestinal dysbiosis, through the TLR7 signaling pathway. *Front Biosci (Landmark Ed)* 2023;28:43. <https://doi.org/10.31083/j.fbl2803043>.
- [11] Huo J, Wang T, Wei B, Shi X, Yang A, Chen D, et al. Integrated network pharmacology and intestinal flora analysis to determine the protective effect of Xuanbai-Chengqi decoction on lung and gut injuries in influenza virus-infected mice. *J Ethnopharmacol* 2022;298:115649. <https://doi.org/10.1016/j.jep.2022.115649>.
- [12] Zhang Q, Luo T, Yuan D, Liu J, Fu Y, Yuan J. Qi-Long-Tian capsule alleviates pulmonary fibrosis development by modulating inflammatory response and gut microbiota. *Funct Integr Genomics* 2023;23:64. <https://doi.org/10.1007/s10142-023-00988-3>.
- [13] Yong W, Zhang L, Chen Y, Li J, Liu Y, Zhang Z. Jianpi Huatan Tongfu granule alleviates inflammation and improves intestinal flora in patients with acute exacerbation of chronic obstructive pulmonary disease. *J Int Med Res* 2020;48:300060520909235. <https://doi.org/10.1177/0300060520909235>.
- [14] Liao Y, Zhong J, Liu S, Dai M, Liu Y, Li X, et al. Yu Ping Feng San for pediatric allergic rhinitis: a systematic review and meta-analysis of randomized controlled trials. *Medicine (Baltimore)* 2021;100:e24534. <https://doi.org/10.1097/MD.00000000000024534>.
- [15] Du Y, Zheng Y, Yu CX, Zhong L, Li Y, Wu B, et al. The mechanisms of Yu Ping Feng San in tracking the cisplatin-resistance by regulating ATP-binding cassette transporter and glutathione S-transferase in lung cancer cells. *Front Pharmacol* 2021;12:678126. <https://doi.org/10.3389/fphar.2021.678126>.
- [16] Bao K, Yuan W, Zhou Y, Chen Y, Yu X, Wang X, et al. A Chinese prescription Yu-Ping-Feng-San Administered in remission restores bronchial epithelial barrier to inhibit house dust mite-induced asthma recurrence. *Front Pharmacol* 2019;10:1698. <https://doi.org/10.3389/fphar.2019.01698>.
- [17] Wang Y, Wang Y, Ma J, Li Y, Cao L, Zhu T, et al. YuPing-FengSan ameliorates LPS-induced acute lung injury and gut barrier dysfunction in mice. *J Ethnopharmacol* 2023;312:116452. <https://doi.org/10.1016/j.jep.2023.116452>.
- [18] Wei Y, Qi M, Liu C, Li L. Astragalus polysaccharide attenuates bleomycin-induced pulmonary fibrosis by inhibiting TLR4/NF- κ B signaling pathway and regulating gut microbiota. *Eur J Pharmacol* 2023;944:175594. <https://doi.org/10.1016/j.ejphar.2023.175594>.
- [19] Cui H, Liu X, Zhang J, Zhang K, Yao D, Dong S, et al. *Rhodiola rosea* L. Attenuates cigarette smoke and lipopolysaccharide-induced COPD in rats via inflammation inhibition and antioxidant and antifibrosis pathways. *Evid Based Complement Alternat Med* 2021;2021:6103158. <https://doi.org/10.1155/2021/6103158>.
- [20] Shi S, Huang D, Wu Y, Pei C, Wang Y, Shen Z, et al. Salidroside pretreatment alleviates PM(2.5) caused lung injury via inhibition of apoptosis and pyroptosis through regulating NLRP3 Inflammasome. *Food Chem Toxicol* 2023;177:113858. <https://doi.org/10.1016/j.fct.2023.113858>.
- [21] Peng M, Li J, Zhou J, Zhang B, Liao J, Yang D, et al. Total alkaloids of *Fritillaria unibracteata* var. *wabuensis* bulbous ameliorate chronic asthma via the TRPV1/Ca(2+)/NFAT pathway. *Phytomedicine* 2023;118:154946. <https://doi.org/10.1016/j.phymed.2023.154946>.
- [22] Pai M, Er-Bu A, Wu Y, Ming TW, Gaun TKW, Ye B. Total alkaloids of bulbous of *Fritillaria cirrhosa* alleviate bleomycin-induced inflammation and pulmonary fibrosis in rats by inhibiting TGF- β and NF- κ B signaling pathway. *Food Nutr Res* 2023;67. <https://doi.org/10.29219/fnr.v67.10292>.
- [23] Liu M, Zhang T, Zang C, Cui X, Li J, Wang G. Preparation, optimization, and in vivo evaluation of an inhaled solution of total saponins of *Panax notoginseng* and its protective effect against idiopathic pulmonary fibrosis. *Drug Deliv* 2020;27:1718–28. <https://doi.org/10.1080/10717544.2020.1856222>.
- [24] Cao B, Xu Z, Liu C, Hu J, Zhu Z, Li J, et al. Protective effects of notoginsenoside R1 on acute lung injury in rats with sepsis. *Ann Transl Med* 2021;9:996. <https://doi.org/10.21037/atm-21-2496>.
- [25] Fu JD, Gao CH, Li SW, Tian Y, Li SC, Wei YE, et al. Atractylenolide III alleviates sepsis-mediated lung injury via inhibition of FoxO1 and VNN1 protein. *Acta Cir Bras* 2021;36:e360802. <https://doi.org/10.1590/ACB360802>.
- [26] Huai B, Ding J. Atractylenolide III attenuates bleomycin-induced experimental pulmonary fibrosis and oxidative stress in rat model via Nrf2/NQO1/HO-1 pathway activation. *Immunopharmacol Immunotoxicol* 2020;42:436–44. <https://doi.org/10.1080/08923973.2020.1806871>.
- [27] Zhang L, Yi H, Jiang D, Li Z. Protective effects of Atractylenolide III on inflammation and oxidative stress in ovalbumin-induced asthma mice and its possible mechanisms. *Gen Physiol Biophys* 2021;40:137–46. https://doi.org/10.4149/gpb_2020046.
- [28] Zare'i M, Rabieepour M, Ghareaghaji R, Zarrin R, Faghfour AH. Nanocurcumin supplementation improves pulmonary function in severe COPD patients: a randomized, double blind, and placebo-controlled clinical trial. *Phytother Res* 2024 Mar;38:1224–34. <https://doi.org/10.1002/ptr.8114>.
- [29] Wu YY, Meng H, Qiao B, Li N, Zhang Q, Jia WQ, et al. Yifei Sanjie formula treats chronic obstructive pulmonary disease by remodeling pulmonary microbiota. *Front Med (Lausanne)* 2022 Jun 29;9:927607. <https://doi.org/10.3389/fmed.2022.927607>.
- [30] Yu JZ, Ying Y, Liu Y, Sun CB, Dai C, Zhao S, et al. Antifibrotic action of Yifei Sanjie formula enhanced autophagy via PI3K-AKT-mTOR signaling pathway in mouse model of

- pulmonary fibrosis. *Biomed Pharmacother* 2019;118:109293. <https://doi.org/10.1016/j.biopha.2019.109293>.
- [31] Sun CB, Ying Y, Wu QY, Liu Y, Yu JZ, Xing HJ, et al. The main active components of *Curcuma zedoaria* reduces collagen deposition in human lung fibroblast via autophagy. *Mol Immunol* 2020;124:109–16. <https://doi.org/10.1016/j.molimm.2020.05.017>.
- [32] Ying Y, Sun CB, Zhang SQ, Chen BJ, Yu JZ, Liu FY, et al. Induction of autophagy via the TLR4/NF- κ B signaling pathway by astragaloside IV contributes to the amelioration of inflammation in RAW264.7 cells. *Biomed Pharmacother* 2021;137:111271. <https://doi.org/10.1016/j.biopha.2021.111271>.
- [33] Yu JZ, Wen J, Ying Y, Yin W, Zhang SQ, Pang WL, et al. Astragaloside trigger autophagy: implication a potential therapeutic strategy for pulmonary fibrosis. *Biomed Pharmacother* 2022;154:113603. <https://doi.org/10.1016/j.biopha.2022.113603>.
- [34] Tveden-Nyborg P, Bergmann TK, Jessen N, Simonsen U, Lykkesfeldt J. BCPT 2023 policy for experimental and clinical studies. *Basic Clin Pharmacol Toxicol* 2023;133:391–6. <https://doi.org/10.1111/bcpt.13944>.
- [35] Mori M, Clausson CM, Sanden C, Jönsson J, Andersson CK, Siddhuraj P, et al. Expansion of phenotypically altered dendritic cell populations in the small airways and alveolar parenchyma in patients with chronic obstructive pulmonary disease. *J Innate Immun* 2023;15:188–203. <https://doi.org/10.1159/000526080>.
- [36] J Y, S W, Y Q, E J, G D, W W, et al. Screening for and combining serum intestinal barrier-related biomarkers to predict the disease severity of AECOPD. *Ann Palliat Med* 2021;10:1548–59. <https://doi.org/10.21037/apm-20-1060>.
- [37] Wang L, Cai Y, Garssen J, Henricks PAJ, Folkerts G, Braber S. The bidirectional gut-lung Axis in chronic obstructive pulmonary disease. *Am J Respir Crit Care Med* 2023;207:1145–60. <https://doi.org/10.1164/rccm.202206-1066TR>.
- [38] Durack J, Lynch SV. The gut microbiome: relationships with disease and opportunities for therapy. *J Exp Med* 2019;216:20–40. <https://doi.org/10.1084/jem.20180448>.
- [39] Zeng X, Yang H, Yang Y, Gu X, Ma X, Zhu T. Associations of clinical characteristics and intestinal flora imbalance in stable chronic obstructive pulmonary disease (COPD) patients and the construction of an early warning model. *Int J Chronic Obstr Pulm Dis* 2021;16:3417–28. <https://doi.org/10.2147/COPD.S330976>.
- [40] Sowah SA, Hirche F, Milanese A, Johnson TS, Grafetstätter M, Schübel R, et al. Changes in plasma short-chain fatty acid levels after dietary weight loss among overweight and obese adults over 50 weeks. *Nutrients* 2020;12. <https://doi.org/10.3390/nu12020452>.
- [41] Wypych TP, Wickramasinghe LC, Marsland BJ. The influence of the microbiome on respiratory health. *Nat Immunol* 2019;20:1279–90. <https://doi.org/10.1038/s41590-019-0451-9>.
- [42] Xue Q, Xie Y, He Y, Yu Y, Fang G, Yu W, et al. Lung microbiome and cytokine profiles in different disease states of COPD: a cohort study. *Sci Rep* 2023;13:5715. <https://doi.org/10.1038/s41598-023-32901-0>.
- [43] Zou YF, Li CY, Fu YP, Feng X, Peng X, Feng B, et al. Restorative effects of inulin from *codonopsis pilosula* on intestinal mucosal immunity, anti-inflammatory activity and gut microbiota of immunosuppressed mice. *Front Pharmacol* 2022;13:786141. <https://doi.org/10.3389/fphar.2022.786141>.
- [44] Aguirre E, Galiana A, Mira A, Guardiola R, Sánchez-Guillén L, García-Pachón E, et al. Analysis of microbiota in stable patients with chronic obstructive pulmonary disease. *APMIS* 2015;123:427–32. <https://doi.org/10.1111/apm.12363>.
- [45] Shi YJ, Huang C, Gong PQ, Liu C, Hu ZQ, Wang H. The protective role of TLR4 in intestinal epithelial cells through the regulation of the gut microbiota in DSS-induced colitis in mice. *Front Biosci (Landmark Ed)* 2023;28:175. <https://doi.org/10.31083/j.fbl2808175>.
- [46] Yang WY, Lee Y, Lu H, Chou CH, Wang C. Analysis of gut microbiota and the effect of lauric acid against necrotic enteritis in *Clostridium perfringens* and *Eimeria* side-by-side challenge model. *PLoS One* 2019;14:e0205784. <https://doi.org/10.1371/journal.pone.0205784>.
- [47] Dickson RP, Erb-Downward JR, Freeman CM, McCloskey L, Falkowski NR, Huffnagle GB, et al. Bacterial topography of the healthy human lower respiratory tract. *mBio* 2017;8. <https://doi.org/10.1128/mBio.02287-16>.
- [48] Vutcovici M, Bittón A, Ernst P, Kezouh A, Suissa S, Brassard P. Inflammatory bowel disease and risk of mortality in COPD. *Eur Respir J* 2016;47:1357–64. <https://doi.org/10.1183/13993003.01945-2015>.
- [49] Lai HC, Lin HJ, Kao YW, Wang KH, Chou JW, Shia BC, et al. Irritable bowel syndrome increases the risk of chronic obstructive pulmonary disease: a retrospective cohort study. *Sci Rep* 2020;10:10008. <https://doi.org/10.1038/s41598-020-66707-1>.